FIELDIANA
Geology

Published by Field Museum of Natural History

New Series, No. 14

THE MAMMALIAN FAUNA OF MADURA CAVE, WESTERN AUSTRALIA PART VI: MACROPODIDAE: POTOROINAE

ERNEST L. LUNDELIUS, JR.

WILLIAM D. TURNBULL

April 30, 1984

Publication 1354

THE MAMMALIAN FAUNA OF MADURA CAVE, WESTERN AUSTRALIA PART VI: MACROPODIDAE: POTOROINAE

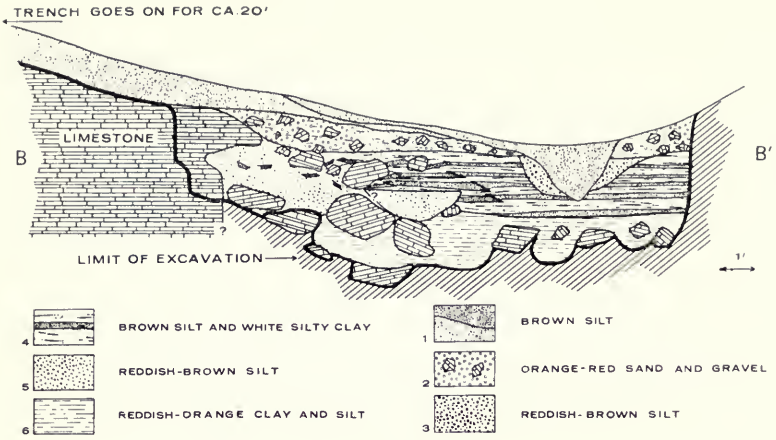
TRENCH GOES ON FOR CA 20'
LIMESTONE
B
B'
LIMIT OF EXCAVATION
1'
4
BROWN SILT AND WHITE SILTY CLAY
5
REDDISH-BROWN SILT
6
REDDISH-ORANGE CLAY AND SILT
1
BROWN SILT
2
ORANGE-RED SAND AND GRAVEL
3
REDDISH-BROWN SILT

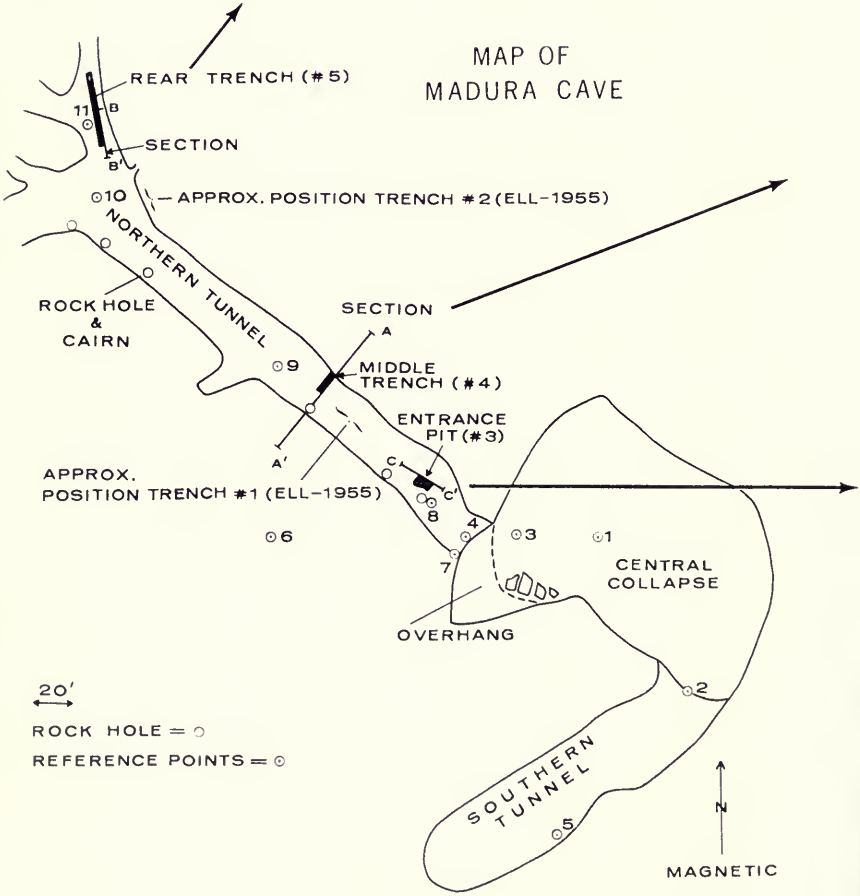
MAP OF
MADURA CAVE
REAR TRENCH (#5)
11
B
SECTION
B'
10
APPROX. POSITION TRENCH #2 (ELL-1955)
NORTHERN TUNNEL
ROCK HOLE
&
CAIRN
SECTION
A
9
MIDDLE
TRENCH (#4)
ENTRANCE
PIT (#3)
A'
C
C'
APPROX.
POSITION TRENCH #1 (ELL-1955)
8
4
6
3
1
7
CENTRAL
COLLAPSE
OVERHANG
2
20'
ROCK HOLE = ○
REFERENCE POINTS = ⊙
SOUTHERN
TUNNEL
5
N
MAGNETIC

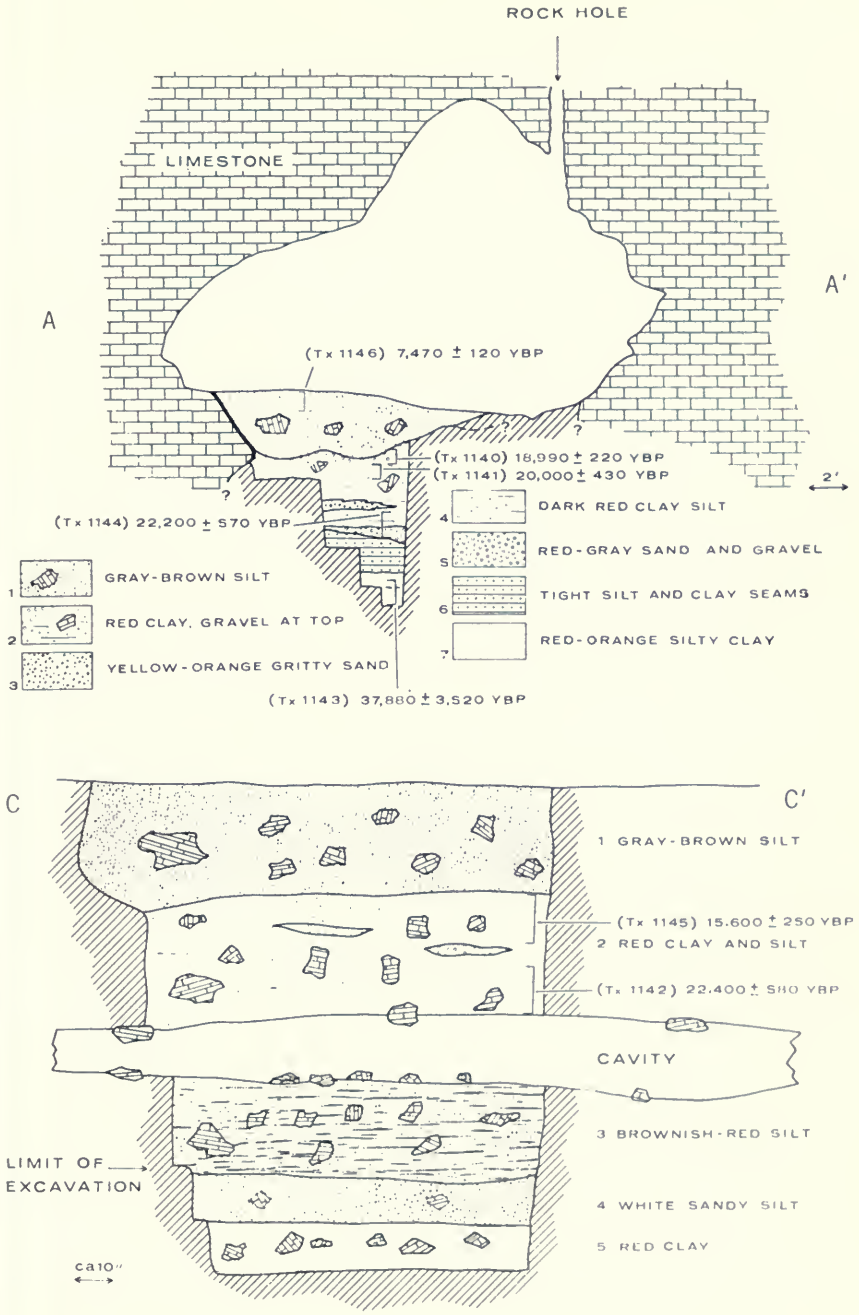

Left, bottom, Map of Madura Cave showing the locations of the trenches. Large arrows point to cross sections of three of the five trenches in the northern tunnel; **left, top,** Trench 5, Section B–B'; **right, top,** Trench 4, Section A–A'; and **right, bottom,** Trench 3, Section C–C'. (All illustrations are taken from Madura Cave, Part I.)

FIELDIANA
Geology

Published by Field Museum of Natural History

New Series, No. 14

THE MAMMALIAN FAUNA OF MADURA CAVE, WESTERN AUSTRALIA PART VI: MACROPODIDAE: POTOROINAE

ERNEST L. LUNDELIUS, JR.

Professor of Geological Sciences
University of Texas at Austin

Research Associate
Department of Geology
Field Museum of Natural History

WILLIAM D. TURNBULL

Curator, Fossil Mammals
Department of Geology
Field Museum of Natural History

Committee on Evolutionary Biology
University of Chicago

Research Associate
Texas Memorial Museum

Accepted for publication July 27, 1983

April 30, 1984

Publication 1354

Library of Congress Catalog Card No.: 72-97564

ISSN: 0096-2651

PRINTED IN THE UNITED STATES OF AMERICA

CONTENTS

LIST OF ILLUSTRATIONS

LIST OF TABLES

ABSTRACT

The potoroines represented in the Madura Cave deposits are *Potorous platyops, Caloprymnus campestris, Bettongia lesueur,* and *Bettongia penicillata.*

Potorous platyops, found in Units 1 through 4–5, is not significantly different from Pleistocene, Holocene, or modern specimens from other parts of Australia.

Caloprymnus campestris, which occurs in all units, shows no significant morphological or size change through the sequence and is smaller than the samples from the Pleistocene of Lake Menindee and from the known Recent material, with no overlap in size.

Bettongia is represented by *B. lesueur,* which is present throughout the stratigraphic sequence, and *B. penicillata,* which is absent only from Unit 7. The Madura Cave *B. lesueur* is smaller in size than other Pleistocene and modern samples, but *B. penicillata* shows no differences.

Today, four species of potoroines are known only from an area near Albany, Western Australia. The presence of *Potorous platyops* suggests that more effective moisture existed in the vicinity of Madura Cave when these sediments were deposited than at present. The association of now allopatric species such as *Potorous platyops* and *Caloprymnus campestris* indicates a more equable climate in the past.

INTRODUCTION

This section of the Madura Cave report covers the rat-kangaroos, Potoroinae, and continues the systematic treatment of the marsupials (Lundelius & Turnbull, 1973, 1975, 1978, 1981, 1982). Measurements, abbreviations, and dental terminology are either those in standard use or those outlined in Parts I through V. Measurements in all tables and graphs are given in millimeters. Headings for the statistical tables are as follows: N, sample size; OR, observed range; M, mean; SE, standard error; SD, standard deviation; CV, coefficient of variation. Abbreviations for institutions are: BMNH, British Museum (Natural History); FMNH, Field Museum of Natural History (Recent mammal); PM, Field Museum of Natural History (fossil mammal); SAM, South Australian Museum; TMM, Texas Memorial Museum; WAM, Western Australian Museum.

Potorous Desmarest, 1804

Potorous platyops (Gould), 1844

Hypsiprymnus platyops Gould, 1844
Potorous platyops Thomas, 1888
Potorous morgani Finlayson, 1938
Potoroops platyops (Tate), 1948

Material

Trench 4, Unit 1
TMM 41106-576, right M_1 (fig. 3B)
TMM 41106-600, left M^1 or M^2 (fig. 2C)
TMM 41106-609, right M_3 (fig. 3F)
TMM 41106-619, right P^4 fragment (fig. 2B)
Trench 4, Unit 2, Level 1
PM 34418, left M^1 or M^2
Trench 4, Unit 2, Level 2
PM 34419, right maxillary fragment with M^3 (fig. 2E)
PM 34420, right M_1 (fig. 3C)
PM 34421, left M^1 or M^2
PM 34422, left M_2 (fig. 3E)
Trench 4, Units 4–5
PM 34423, left M^1 or M^2 (fig. 2D)
TMM 41106-647, juvenile ramus with I, P_4, alveoli of P_3, dP_4, M_1 (fig. 3A)
PM 34424, right M_1
PM 34425, right M_1 (fig. 3D)
WAM 75.1.130, left M^1 or M^2
Trench 5, Unit 4
PM 34426, right M^1 or M^2
Trench 5, Unit 6
WAM 75.1.131, left M^1 or M^2
TMM 41106-632, right dP^4 (fig. 2A)

Comparative Material

Potorous platyops
BMNH 46.4.25.11, *P. platyops* type
BMNH 53.10.22.19
SAM P168, *P. morgani* cotype
Hastings' Cave
PM 6313 (fig. 1D,E), 6314–6318, 6695, 7073–7078, 36844–36848, 36852, 36869–36871
Wedge's Cave
PM 5598–5602, 36843
Webb's Cave
PM 4355 (fig. 1A–C)

Description

Upper Dentition.—The dP^4 (TMM 41106-632; fig. 2A) is rooted, but unworn. Its nearly equally spaced cusps and primary lophs are low and sharp. The tooth is rectangular in outline with the anterior ridge of the paracone extending forward as a short blade. As compared with PM 6313 (fig. 1D,E) and PM 6315, the Madura Cave specimen is more elongate with more pronounced constrictions both labially and lingually between the protoloph and metaloph. A low

TABLE 1. Measurements of upper dentitions of *Potorous platyops* from Madura Cave.

Teeth	Specimen No.	Length	Anterior width	Posterior width
dP^4	TMM 41106-632	2.85	2.13	2.20
P^4	TMM 41106-619	> 3.5	> 1.7	1.62
M^1 or M^2	TMM 41106-600	3.42	2.96	2.74
	PM 34423	3.34	3.04	2.89
	PM 34424	3.45	2.96	2.81
	PM 34421	3.08	3.00	2.81
	PM 34426	3.42	2.04	2.70
	PM 34418	3.12	...	2.74
	WAM 75.1.130	3.04	2.74	2.66
	WAM 75.1.131	3.34	2.81	2.74
M^3	PM 34419	3.12	2.74	2.25

angular ridge extends posteriorly from the apex of the protocone parallel to the labial side of the tooth. This ridge almost reaches the median valley, then swings abruptly lingually and disappears. A similar low ridge runs anteriorly from the apex of the metacone along the labial edge of the tooth and disappears near the valley without turning lingually. Low, blunt, and more massive ridges connect the protocone and hypocone, meeting at a nearly right-angled V where they cross the bottom of the median valley. The protoloph forms a broadly open saddle, with the paracone making the greater contribution. The metaloph is nearly straight and horizontal. It is weakly notched near the hypocone. The metacone causes the labial half of the metaloph to bulge posteriorly. The postcingulum is a heavy ridge, especially near the hypocone. It is U-shaped in posterior view and it and the metaloph delimit a shallow, crescentic posterior cingular basin.

The P^4 (TMM 41106-619) lacks the anterior end. It is unworn, lacks roots, and probably was unerupted (fig. 2B). The long axis of the tooth is concave labially. This appears to be a variable character since PM 4355 (fig. 1A–C) from Webb's Cave (about 55 miles [89 km] east of Madura Cave) is nearly straight, while PM 6313 (fig. 1D–E) and PM 6315 from Hastings' Cave show considerable difference in their curvature. Of all the specimens here compared, PM 6315 shows the most curvature. The anterior cusp is higher than the others. The two specimens from the Nullarbor Plain differ from the two Hastings' Cave specimens in having less pronounced vertical ridges on the labial side of the two anterior cusps.

It is difficult to distinguish between isolated M^1s and M^2s. The M^1 in most of the available comparative material has a more pronounced anterolabial projection on the procingulum than does the M^2. However, the Madura Cave specimens do not fall into two distinct groups on the basis of this character or on the basis of size. Both M^1 and M^2 probably are represented. There is much more similarity between M^1 and M^2 in the Madura Cave sample than in the Hastings' Cave and Wedge's Cave samples.

The M^1 or M^2 (as represented by TMM 41106-600; fig. 2C) is slightly longer than wide. The posterior part of the tooth is narrower than the anterior part, both in the spacing of the two posterior cusps with respect to the anterior ones and in the overall width of the tooth. Its protocone and hypocone are relatively

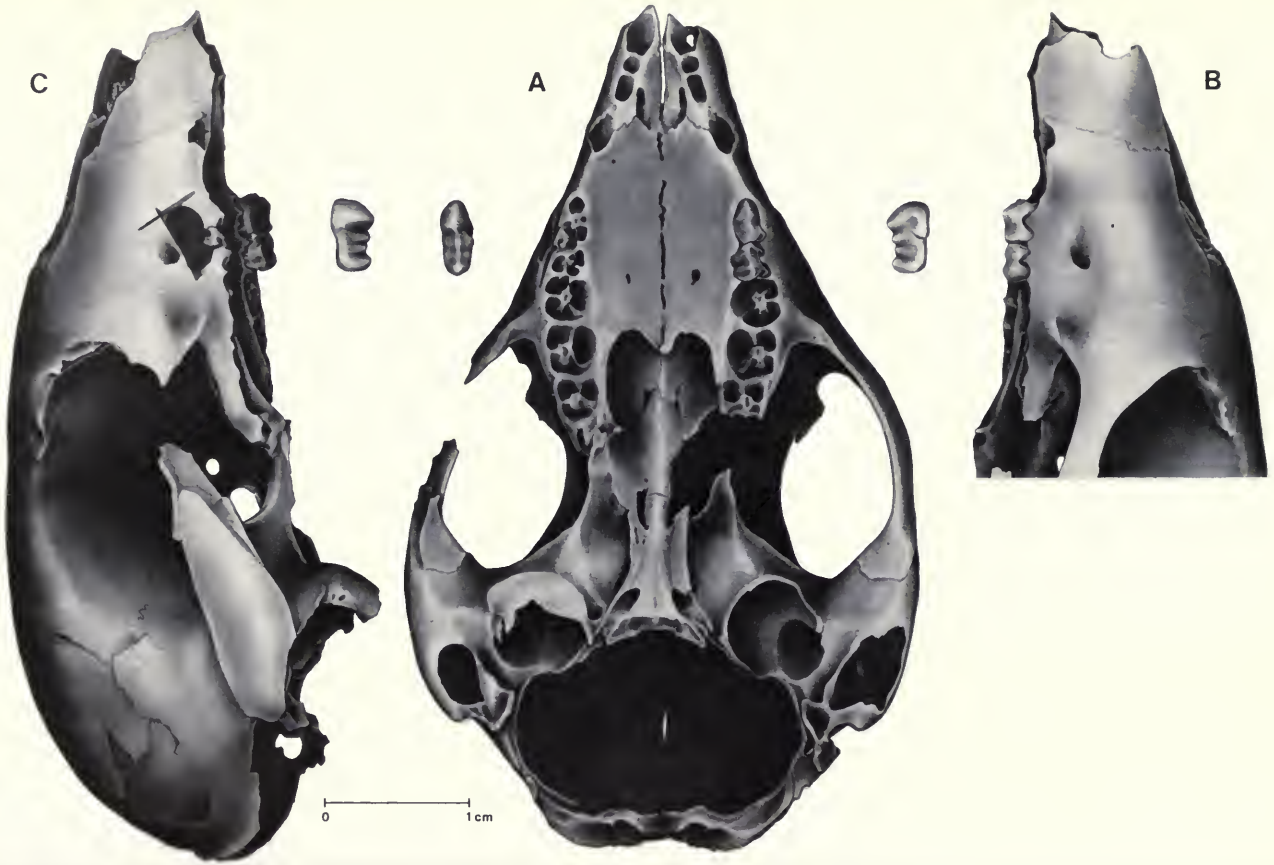
C
A
B
0
1 cm

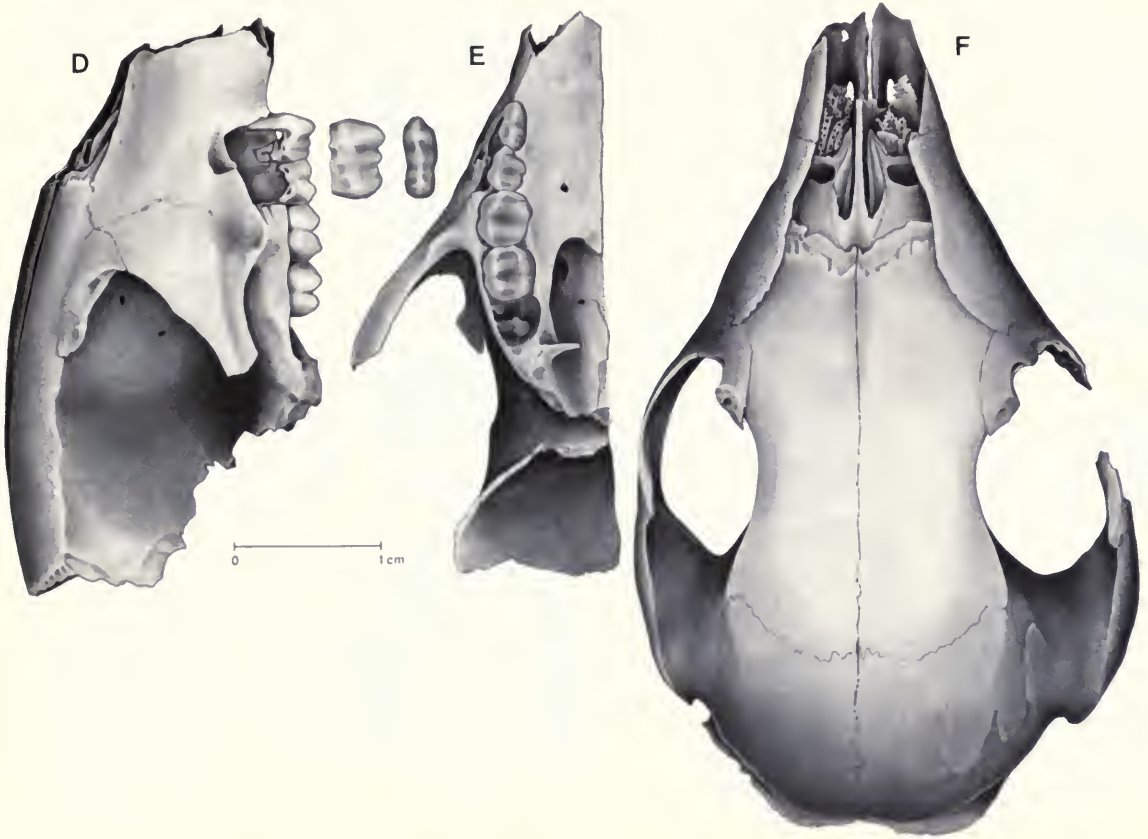

FIG. 1. *Potorous platyops* comparative materials. **A–C,F,** PM 4355. Recent skull from surface of Webb's Cave, Western Australia. **A,** Ventral view with unerupted right P^4 removed from crypt and shown in occlusal view. **B,** Left lateral view of maxillary region with right P^4 removed from its crypt and shown in lingual view. **C,** Right lateral view showing lingual view of left P^3 and dP^4 and right P^4 removed from its crypt and shown in labial view. **F,** Dorsal view. **D,E,** PM 6313. Subrecent partial skull from Hastings' Cave, Western Australia. **D,** Right lateral view with P^4 removed from its crypt. **E,** Ventral view of right side with P^4 removed from its crypt and shown in occlusal view.

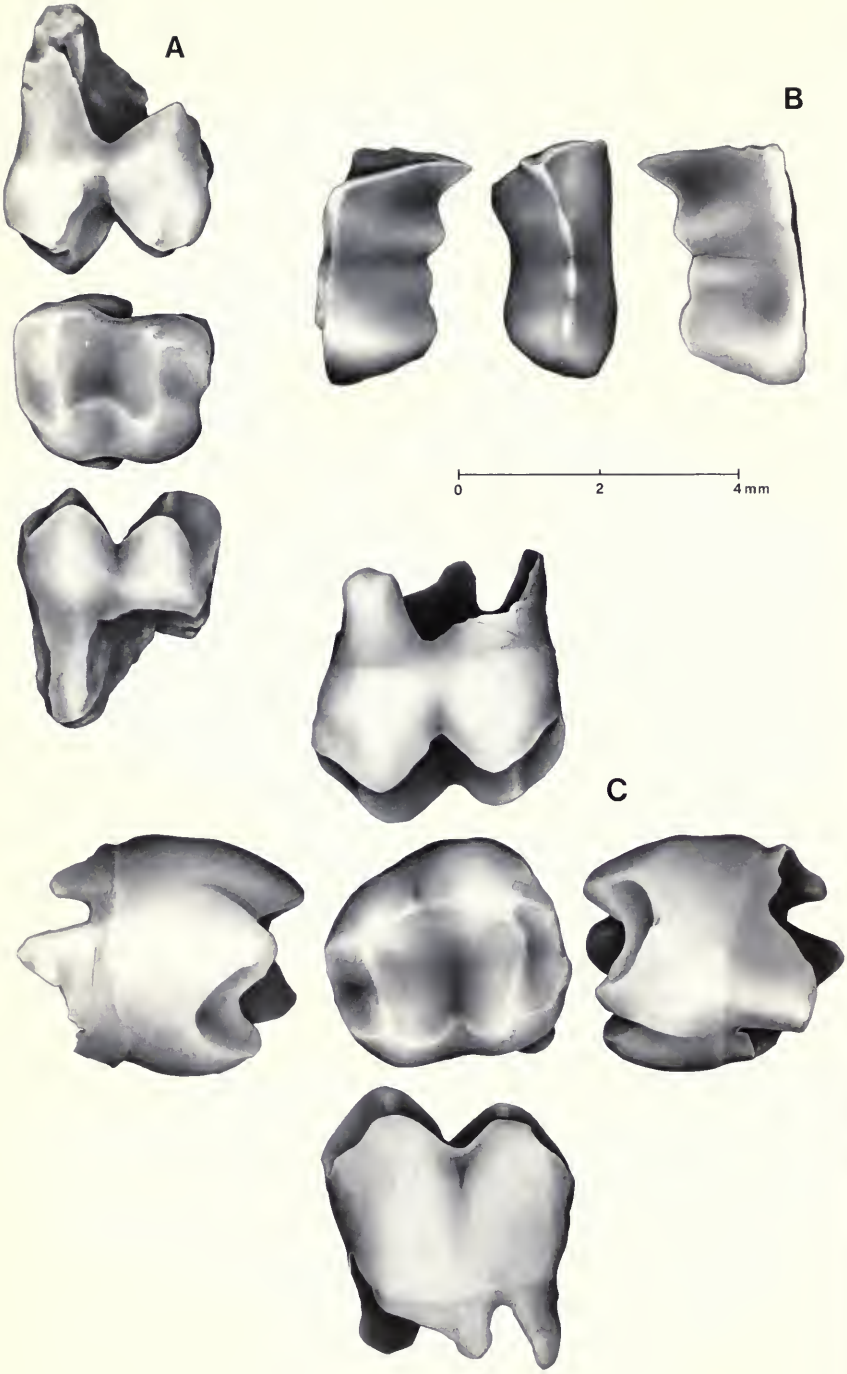

FIGURE 2.

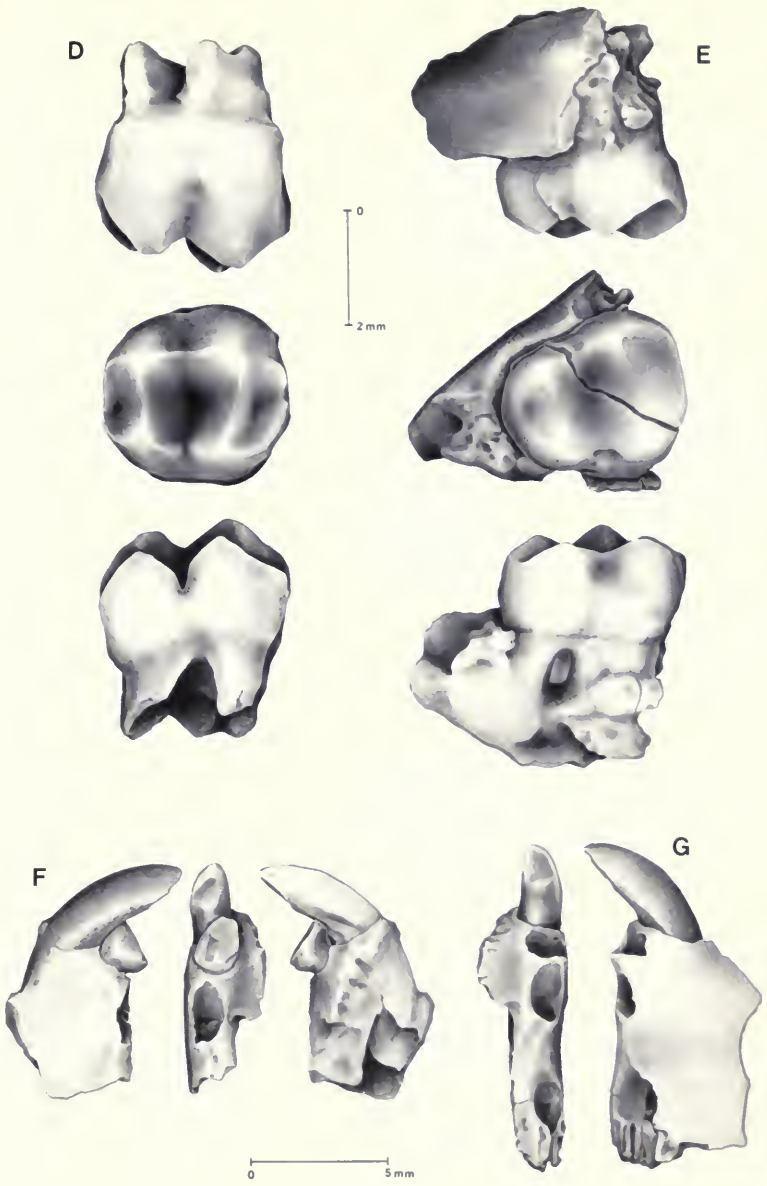

FIG. 2. **A-E,** *Potorous platyops* from Madura Cave. **A,** TMM 41106-632. Right dP^4 shown in labial (top), crown, and lingual views. **B,** TMM 41106-619. Right P^4 shown in labial (left), crown, and lingual views. **C,** TMM 41106-600. Left M^1 or M^2 shown in labial (top), crown, lingual, posterior (left), and anterior views. **D,** PM 34423. Left M^1 or M^2 shown in labial (top), crown, and lingual views. **E,** PM 34419. Right M^3 in maxillary fragment shown in labial (top), crown, and lingual views. **F,G,** *Incertae sedis,* probably *P. platyops,* Madura cave. **F,** TMM 41106-682. Right premaxillary with I^{1-2}, alveolus for I^3, shown in labial (left), crown, and lingual views. **G,** PM 34510. Left premaxillary with I^1, alveoli for I^{2-3}, and C, shown in crown and labial views.

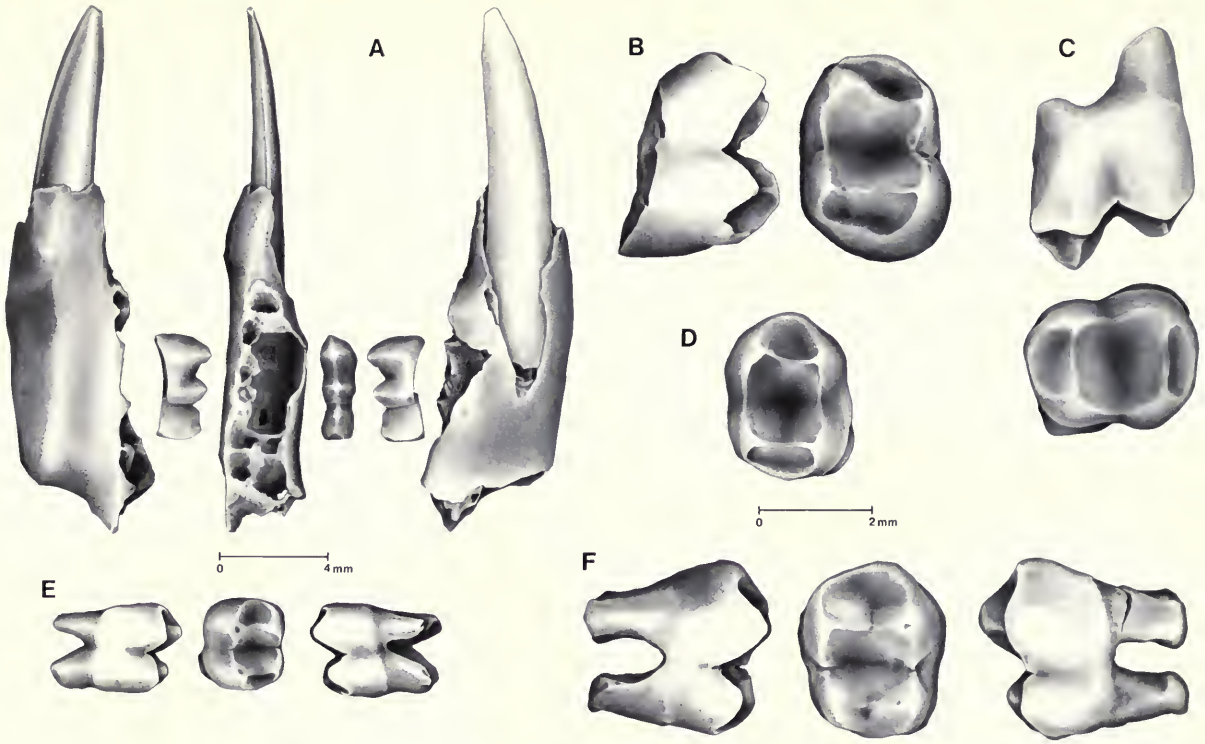

FIG. 3. *Potorous platyops* from Madura Cave. **A,** TMM 41106-647. Right ramus with I and P_4 (removed from crypt) shown in lingual (left), dorsal, and labial views. **B,** TMM 41106-576. Right M_1 shown in crown and labial views. **C,** PM 34420. Right M_1 shown in crown and labial views. **D,** PM 34425. Right M_1 shown in crown view. **E,** PM 34422. Left M_2 shown in lingual (left), crown, and labial views. **F,** TMM 41106-609. Right M_3 shown in lingual (left), crown, and labial views.

TABLE 2. Measurements of lower dentitions of *Potorous platyops* from Madura Cave.

Teeth	Specimen No.	Length	Anterior width	Posterior width
P_4	TMM 41106-647	3.80	1.34	1.14
M_1	PM 34420	3.01	2.13	2.20
	PM 34425	2.96	1.98	2.05
	TMM 41106-576	3.34	2.37	3.43
M_2	PM 34422	3.27	2.74	2.58
M_3	TMM 41106-609	3.08	2.37	2.09

high, blunt cusps. The metaloph is nearly straight, but the protoloph is slightly bowed and lies slightly oblique to the long axis of the tooth, joining the protocone at its anterior margin. In profile the crests of the lophs are gently concave between the cusps. A low but continuous crest connects the protocone to the hypocone. Crests from the paracone and metacone nearly meet at the bases of these cusps. These crests and the lophs define a nearly square, almost featureless central basin. Pro- and postcingula are both present. The procingulum is connected to the protocone by a weak crest and to the paracone by a somewhat stronger crest, forming a broad asymmetrical basin. Similarly developed distinct crests extend downward and posteriorly from the apices of the hypocone and metacone, meeting about halfway to the base of the crown to form a symmetrical posterior cingular basin (fig. 2C). The other three M^1s or M^2s (PM 34423, PM 34424, WAM 75.1.131) show minor variations in the condition of the notch that separates the crests from the paracone and metacone. PM 34423 (fig. 2D) and PM 34424 have a narrow U-shaped notch, while WAM 75.1.131 has a narrow cleft. Wear has made it impossible to determine the condition of this feature in TMM 41106-600. Specimen PM 34423 differs from the other three M^1s or M^2s in possessing a protoloph that in profile has an open V shape rather than a U shape. This character may be affected by wear. The posterior cingular basins of PM 34423 and WAM 75.1.131 are narrower than those of TMM 41106-600 and PM 34424.

The M^3 (PM 34419) differs from the M^1s and M^2s in having the posterior part of the tooth distinctly narrower than the anterior part. It has a square, featureless central basin, a broad, asymmetrical procingular basin, and a well-defined oval posterior cingular basin (fig. 2E).

No M^4s have been recognized.

Lower Dentition.—The mandible (TMM 41106-647; fig. 3A) is shallow. The lower incisor is narrow and procumbent, as is normal in *Potorous*, and is curved inward and upward throughout its length. It shows slight wear at the tip and on the ventromedial edge. The ventrolateral surface of the tooth is convex and enamel covered throughout its length. In cross section the dorsolateral surface is generally convex in its dorsal half, with a narrow groove on its dorsal edge. A broad trough extends the length of the tooth on the ventromedial edge. Enamel is present only on the distal end of the medial convexity. There do not appear to be any differences between the Madura tooth, the Western Australian specimens of *P. platyops*, and the Kangaroo Island *P. morgani* which cannot be accounted for by individual variation.

All the cheek teeth except the unerupted P_4 have been lost from the mandible. The crown of the P_4 (fig. 3A) is well formed but the tooth lacks roots.

TABLE 3. Measurements of upper dentitions of various samples of fossil and Recent *Potorous platyops*.

		Hastings' Cave								Wedge's Cave							Recent			
		PM 6313	PM 6314	PM 6315	PM 36847	PM 36845	PM 36844	PM 36852	Mean	PM 5598	PM 5599	PM 5600	PM 5601	PM 36843	PM 5602	Mean	Webb's Cave PM 4355	Walyema Swamp BMNH 46.4. 25.11 Type	Albany, W.A. BMNH 53.10. 22.19	*Potorous morgani* Cotype SAM P 168
P^3	L	3.19	···	3.19	···	···	···	3.12	3.17	···	2.66	···	···	···	···	2.66	2.74	···	···	···
	AW	1.52	···	1.60	···	···	···	1.52	1.55	···	.95	···	···	···	···	.95	1.67	···	···	···
	PW	1.82	···	1.71	···	···	···	1.60	1.71	···	1.52	···	···	···	···	1.52	1.75	···	···	···
dP^4	L	2.89	···	2.74	···	···	···	···	2.28	···	2.66	···	···	···	···	2.66	2.51	···	···	···
	AW	2.17	···	2.36	···	···	···	···	2.27	···	2.24	···	···	···	···	2.24	1.98	···	···	···
	PW	2.13	···	2.28	···	···	···	···	2.21	···	2.13	···	···	···	···	2.13	1.90	···	···	···
P^4	L	5.36	···	5.02	4.44	4.10	5.17	···	4.82	4.64	4.83	5.02	4.64	···	5.56	4.94	4.64	4.5	4.7	4.9
	AW	1.98	···	2.05	1.52	1.48	1.98	···	1.80	1.98	2.05	1.82	1.75	···	···	1.90	2.05	···	···	···
	PW	1.87	···	1.94	1.29	1.52	1.75	···	1.67	2.01	1.90	···	1.60	···	···	1.84	1.75	···	···	···
M^1	L	3.65	3.27 (w)	3.42	···	···	···	···	3.45	3.12 (w)	3.65	3.34 (w)	3.19 (w)	3.34	>3.12 (w)	3.29	···	···	···	···
	AW	3.27	3.04 (w)	3.34	···	···	···	···	3.22	3.12 (w)	3.19	3.19	2.81	2.84	···	3.03	···	···	···	···
	PW	3.00	2.58 (w)	2.96	···	···	···	···	2.85	2.96 (w)	2.96	2.81	2.51	2.51	···	2.75	···	···	···	···
M^2	L	3.65	3.28 (w)	···	···	···	···	···	3.47	3.42 (w)	3.57	3.34 (w)	3.34 (w)	3.34 (b)	···	3.40	···	···	···	···
	AW	3.27	2.89 (w)	···	···	···	···	···	3.08	3.34 (w)	3.42	3.50	2.81	···	···	3.27	···	···	···	···
	PW	3.04	2.74 (w)	···	···	···	···	···	2.89	2.96 (w)	3.12	3.17	2.51	···	···	2.94	···	···	···	···
M^3	L	···	2.74	3.00	···	···	···	···	2.87	2.89 (w)	···	3.17 (w)	2.66 (w)	···	···	2.91	···	···	···	···
	AW	···	2.46	2.76	···	···	···	···	2.61	2.96 (w)	···	2.84	2.28	···	···	2.69	···	···	···	···
	PW	···	2.13	2.32	···	···	···	···	2.23	2.43 (w)	···	2.51	2.13	···	···	2.36	···	···	···	···

TABLE 4. Measurements of lower dentitions of fossil and Recent samples of *Potorous platyops*.

		Hastings' Cave															Recent		
		PM 6316	PM 6317	PM 6318	PM 6695	PM 7073	PM 7074	PM 7075	PM 7076	PM 7077	PM 7078	PM 36846	PM 36848	PM 36869	PM 36870	PM 36871	Mean	Walyema Swamp BMNH 46.4. 25.11 Type	Albany, W.A. BMNH 53.10. 22.19	*Potorous morgani* Cotype SAM P 168
P_3	L	...	...	...	...	2.43	2.81	2.74	...	...	...	...	...	...	...	...	2.66	...	...	...
	AW	...	...	...	...	1.29	1.44	1.37	...	...	...	...	...	...	...	...	1.37	...	...	...
	PW	...	...	...	...	1.44	1.52	1.14	...	...	...	...	...	...	...	...	1.37	...	...	...
dP_4	L	...	...	...	3.04	2.20	2.58 (w)	2.43	...	...	...	...	2.36	...	...	...	2.52	...	...	...
	AW	...	...	...	1.60	1.26	1.52	1.22	...	...	...	...	1.52	...	...	...	1.42	...	...	...
	PW	...	...	...	1.98	1.52	1.86	1.33	...	...	...	...	1.82	...	...	...	1.70	...	...	...
P_4	L	...	4.33	...	...	3.88 (u)	4.56 (u)	4.33 (u)	4.18	...	4.03 (u)	4.03 (u)	...	4.10	4.18	...	4.18	3.8	4.1	4.2
	AW	...	1.86	...	...	1.26	1.52	1.52	1.63	...	1.37	1.37	...	1.90	1.67	...	1.57	...	...	...
	PW	...	1.67	...	...	1.22	1.60	1.52	1.67	...	1.29	1.22	...	1.90	1.82	...	1.55	...	...	...
M_1	L	3.19 (w)	3.30 (w)	...	...	...	3.34	...	3.34	3.19	...	...	...	2.96 (w)	3.19 (w)	3.12 (w)	3.20	...	...	...
	AW	2.20	2.36	...	...	...	2.28	...	2.28	2.13	...	...	...	2.24	2.43	2.36	2.29	...	...	[illegible]
	PW	2.51	2.58	...	...	...	2.51	...	2.43	2.36	...	...	...	2.36	2.66	2.58	2.50	...	...	[illegible]
M_2	L	3.53 (w)	3.57 (w)	3.57 (u)	...	...	3.72	...	...	...	...	...	...	3.30 (w)	3.42 (w)	3.50	3.52	...	...	[illegible]
	AW	2.66	2.89	2.70	...	...	2.85	...	...	...	...	...	...	2.70	2.89	2.96	2.81	...	[illegible]	[illegible]
	PW	2.74	2.81	2.74	...	...	2.66	...	...	...	...	...	...	2.58	2.81	2.74	2.73	...	[illegible]	...
M_3	L	...	3.27 (w)	...	...	...	3.19	3.12 (u)	3.12 (u)	3.16 (u)	...	...	...	3.04	3.19	...	3.16	...	...	...
	AW	...	2.74	...	...	...	2.66	2.58	2.51	2.36	...	...	...	2.51	2.74	...	2.59	...	...	...
	PW	...	2.43	...	...	...	2.36	2.20	2.28	2.20	...	...	...	2.28	2.43	...	2.31	...	...	[illegible]

The long axis of the tooth is straight, in contrast to the situation in P^4. The tooth is compressed and divided on both sides by two broad grooves into three well-defined cusps. The posterior cusp has an indistinct groove that forms a low notch on the crest. The posterior end of the tooth is very flat. The length of the P_4 is 3.80 mm, which is just below the size range of P_4s of a sample of *P. platyops* from Hastings' Cave, Western Australia (table 3). The type (BMNH 46.4.25.11, female) and one additional Recent specimen from Western Australia (BMNH 53.10.22.19, male) measure 3.8 and 4.1 mm, respectively. The length of the P_4 of one of the cotypes of *Potorous morgani* is 3.9 mm (Finlayson, 1938, p. 134).* An examination of Tables 2 and 4 shows that the lengths of the P_4s of all available samples of *P. platyops*, both fossil and Recent, overlap the sample from Hastings' Cave.

The M_1 (as represented by TMM 41106-576; fig. 3B) is slightly narrower across the protolophid than across the metalophid (the protolophid and metalophid are more nearly equal in PM 34420). The central basin is large, longer on the lingual than the labial side, with no significant irregularities. Labial and lingual ridges connect the protoconid and hypoconid and the metaconid and entoconid along the margins of the tooth. In TMM 41106-576 these ridges are not fused where they meet; in PM 34420 and PM 34425 the ridges are fused, with no sign of a cleft. The pro- and postcingula are distinct and are connected with the apices of their associated cusps. The anterior and posterior cingular basins are asymmetrical with their centers labial to the midline of the tooth. In TMM 41106-576 the posterior cingular basin is subdivided by a low bulge on the floor of the basin; this feature is lacking in the other two M_1s, and PM 34420 has a more symmetrical posterior cingular basin.

The only M_2 (PM 34422; fig. 3E) is rectangular with the metalophid slightly narrower than the protolophid. The ridges from the major cusps join along the sides of the central basin without fusing, as in TMM 41106-576. The posterior cingular basin is smaller than that in M_1 and is more lingually situated.

The only M_3 (TMM 41106-609; fig. 3F) is moderately worn. It is slightly wider across the protolophid than across the hypolophid, its central basin is nearly square, and there is a trace of a transverse valley across the middle, as in M_1. Wear has reduced the ridges labial and lingual to the central basin, but the clefts are still in evidence where the ridges meet but remain unfused. The procingulum is expanded anteriorly in its middle, so that the anterior cingular basin is more oval than in the M_1 but lacks the prominent anterolabial cuspule seen in PM 7074 from Hastings' Cave. Wear has truncated the postcingulum to the point where the basin is nearly obliterated. Only a small, deep pit remains almost directly behind the saddle of the hypolophid. The thick enamel tips of the protoconid and hypoconid have both been breached by wear so that small circles of dentine are exposed.

Discussion

The dentition of *Potorous platyops* differs from that of other species of *Potorous* primarily in its smaller size. The P^4 of *P. platyops* differs from that of *P. tridac-*

* The measurement is listed as P^4. This, as well as the references to M^1 through M^4, is surely a typographical error, as the paragraph on p. 134 refers to the mandible, and the length of P^4 in the table on p. 139 is 5.0 mm.

tylus (including *P. gilberti*) in having a shallower notch between the second and third cusps and the absence of a flared base. Three specimens of *Potorous apicalis* from Tasmania (FM 98902, FM 57805, FM 98789) differ from *P. platyops* in having three or four small cusps between the two large end ones rather than the two characteristic of *P. platyops*.

This is the fifth reported occurrence of *P. platyops* in cave deposits on the Nullarbor Plain. The species was reported earlier from Webb's Cave (55 miles [89 km] east of Madura) on Mundrabilla Station (Lundelius, 1963) and more recently (Butler & Merrilees, 1971) from caves near Madura, Eucla, and Koonalda. The material from the older deposits of Madura Cave shows that the species occupied the Nullarbor Plain during the latter part of the Pleistocene.

Lundelius (1963) suggested that it is likely that *P. platyops* from Western Australia, *P. morgani* from Kangaroo Island, and the specimen from Webb's Cave are representatives of a single species, *P. platyops*. The extensive overlap in dental dimensions of the various samples of *P. platyops* (including the cotypes of *P. morgani*) supports this view. Finlayson (1938) listed six characters as criteria which separated the type of *P. platyops* from *P. morgani*. Four of these are minor differences in proportions which Finlayson himself pointed out might break down if larger series of specimens were examined. The other two, the size and shape of the first upper incisor and the degree of specialization of the lower incisor, seem to us to be equally subject to geographic variation, although little material from Madura Cave bears on this.

Potorous platyops formerly was widespread in coastal southern Australia. In addition to the Madura Cave Pleistocene and Holocene fossils reported here, and to the Webb's Cave and Kangaroo Island occurrences discussed above, *P. platyops* is also known from Pleistocene deposits in Victoria Cave, southeastern Southern Australia (Smith, 1971), and from the following Holocene deposits: Dongara-Hill River area on the west coast of Western Australia (Lundelius, 1957, 1960), Bremer Bay on the south coast of Western Australia (Butler & Merrilees, 1971), several caves on the Nullarbor Plain (Lundelius, 1957, 1963; Butler & Merrilees, 1971), and from aboriginal sites on the lower Murray River (Wakefield, 1964). Several of these occurrences indicate a late Holocene age for the specimens: the Webb's Cave specimen was collected from the surface (Lundelius, 1963); the Wedge's Cave material from the west coast is known to be younger than 3750 BP; the Bremer Bay material has C^{14} dates indicating an age between 1190 and 620 BP; the material from caves near Madura, Eucla, and Koonalda all appears to be of late Holocene age (Butler & Merrilees, 1971); and the species is represented in the lower Murray River sites with C^{14} dates of 1800 BP. Evidently *P. platyops*, like *Cercartetus concinnus* (Lundelius & Turnbull, 1982), persisted until quite recently, perhaps as relict populations in locally favorable areas. The restriction and fragmentation of the mainland population probably resulted from the post-Pleistocene trend toward aridity.

Potorous *Incertae Sedis*

Material

Trench 3, Unit 2, Level ?

TMM 41106-682, premaxillary fragment with I^{1-2}, alveolus of I^3 (fig. 2F)

Trench 4, Unit 2, Level 1
PM 34510, premaxillary fragment with I^1, alveoli for I^{2-3}, C (fig. 2G)
PM 36877, 36878, two I^1s
Trench 5, Unit 6
PM 38673, I^1

Description

These specimens probably belong to *Potorous platyops*. The available comparative specimens have no upper incisors preserved; hence, the uncertainty. The I^1s thought to belong to *Potorous* are uniformly curved, nearly prismatic teeth with only a slight taper throughout their length. If not too worn, they may have a faint groove on their posterolabial edges. The I^1s lack enamel on their posterior side except at the extreme labial edge where it folds around from the labial side. The I^2 has an oval crown in occlusal view. The occlusal surface is flat. The crown is expanded forward so that more of it lies anterior to the root than posterior to it. The alveolus for the canine lies largely within the premaxillary, and the anterior edge of the incisive foramen is located opposite the alveolus for I^3.

Caloprymnus Thomas, 1888

Caloprymnus campestris (Gould), 1843
Bettongia campestris Gould, 1843

Material

Trench 3, Unit 2, Level 1
TMM 41106-160, left ramus with P_3, dP_4, M_{1-2}, alveoli for M_{3-4} (fig. 5A)
TMM 41106-161, right ramus with P_3, dP_4, M_{1-3}, alveoli for M_4 (fig. 5B)
TMM 41106-162, right ramus with shattered roots of all teeth
TMM 41106-163, left ramus with I, P_{3-4} removed, M_{1-3} (fig. 5C)
TMM 41106-164, left ramus fragment with P_4, M_1 (fig. 5D)
TMM 41106-165, right ramus fragment with worn M_2
TMM 41106-166, left ramus with P_4, M_{2-4} (fig. 5E)
TMM 41106-167, left maxillary fragment with P^3, dP^4, P^4 in crypt, M^{1-2}, alveoli for M^3 (fig. 4C)
TMM 41106-304, right maxillary fragment with M^{1-2}
TMM 41106-305, right maxillary fragment with M^{1-3}
TMM 41106-306, left maxillary fragment with M^{1-2}
TMM 41106-307, left maxillary fragment with worn M^{1-2} (fig. 4F)
TMM 41106-308, right maxillary fragment with P^4 broken, M^1
TMM 41106-309, right maxillary fragment with worn M^{3-4} (fig. 4G)
TMM 41106-310, right maxillary fragment with P^4–M^1 (fig. 4D)
TMM 41106-313, left M_2 or M_3
TMM 41106-2829, left M^2, M^1, or M^3
TMM 41106-2830, -5099, two right M_3s or M_2s
TMM 41106-5100, M_2 or M_1 or M_3
TMM 41106-5101, right M_2
TMM 41106-5102, right M_1
TMM 41106-5103, left M^2, M^1, or M^3
TMM 41106-5104, right M^1 or M^2
TMM 41106-5105, left M^1 or M^2
TMM 41106-5106, right M_2 or M_3
TMM 41106-5107, right M^1 or M^3
TMM 41106-5108, left dP_4

TMM 41106-5120, left P_4
TMM 41106-5122, left P^4
TMM 41106-5123, left P_4
TMM 41106-5124, posterior ¾ right P_4
TMM 41106-5125, -5126, two right dP_4s
TMM 41106-5127, badly worn lower molar
TMM 41106-5128, right M^2 or M^1
TMM 41106-5129, right dP_4
WAM 75.1.145, left M^1 or M^2
PM 34427, right maxillary fragment with M^{1-2}
PM 34428, left maxillary fragment with P^3, dP^4
PM 34429, left maxillary fragment with M^{1-2}
PM 34430, right M_1 or M_2
PM 34431, 34432, two left dP^4s
PM 34433, right maxillary fragment with P^4 in crypt
PM 34435, left ramus with all teeth shattered
PM 34461, right ramus fragment with I_1, P_4
PM 34462, left ramus fragment with P_4–M_3
PM 34463, edentulous right ramus
PM 34464, left ramus with M_3
PM 34465, right ramus fragment with I_1, P_3
PM 34466, right ramus fragment with I_1, M_{2-3}, crypt for P_4
PM 34467, right ramus fragment with M_{2-3}
PM 34468, right ramus fragment with M_{2-3} or M_{3-4}
PM 34470, edentulous maxillary fragment with alveoli for dP^4–M^1, crypt for P^4

Trench 3, Unit 2, Level 2
PM 34436, right maxillary fragment with alveoli for P^3, dP^4, crypt for P^4

Trench 3, Unit 2, Level 4
WAM 75.1.132, left M_1
WAM 75.1.133, left M_2 or M_3
PM 34437, 34438, two right P^3s
PM 34439, posterior ⅔ right P^3
PM 34440, right P^3
PM 34441, 34442, two right dP^4s
PM 34443, right P^4
PM 34444, left P_4
PM 34445, right dP_4
PM 34446, right M_1
PM 34447, left M_1
PM 34448, right M^1
PM 34449, right M^2
PM 34450, very worn left M^2
PM 34451, right M^1
PM 34452, left M_1
PM 34453, right M^2
PM 34454, right M_1
PM 34455, left M_2 or M_3
PM 34456, right M^2 or M^3
PM 34457, 34458, two left M^1s or M^2s
PM 34459, right M^2, M^1, or M^3
PM 34460, right M_2 or M_1

Trench 3, Unit 3, Level ?
TMM 41106-34, maxillary with P^3, P^4 removed from crypt, M^{1-2} (fig. 4B)
TMM 41106-35, left dP^4
TMM 41106-36, left ramus fragment with M_1, alveolus for M_2, part of crypt for P_4
TMM 41106-311, right ramus fragment with M_{3-4}
TMM 41106-312, left ramus fragment with M_2 broken, M_3
TMM 41106-344, left ramus with I, P_3, dP_4, P_4 in crypt, M_{1-2}
TMM 41106-345, left ramus with dP_4, M_{1-2}, unerupted P_4 and M_{3-4}
TMM 41106-346, left ramus with P_3, dP_4
TMM 41106-348, edentulous left ramus fragment

TMM 41106-349, left ramus fragment with dP_4, M_{2-3}
TMM 41106-351, right ramus with M_1
TMM 41106-352, right ramus with I, dP_4, M_1
TMM 41106-353, right ramus with M_2
TMM 41106-354, left ramus with dP_4–M_1
TMM 41106-357, right maxillary with P^3, dP^4, M^{1-2}
TMM 41106-358, right maxillary with M^{2-3} (fig. 4E)
TMM 41106-359, left maxillary with P^3, dP^4, M^{1-2}
WAM 75.1.134, left ramus with I_1 broken, alveoli for P_3, dP_4, M_{1-2}
WAM 75.1.146, right ramus fragment with dP_4, P_4 in crypt, alveoli for I, P_3, M_{1-2}
WAM 75.1.147, right ramus fragment with P_4 exposed in crypt, alveoli for P_3–M_1
PM 34471, 34472, two left dP^4s
PM 34473, right M^2 or M^3
PM 34474, right M^2
PM 34475, edentulous right ramus fragment
PM 34476, juvenile edentulous left ramus
PM 34477, left maxillary fragment with very worn M^{1-2}
PM 34478, right ramus fragment with I_1, P_3
PM 34479, edentulous left ramus
PM 34480, edentulous right ramus
PM 34481, right ramus with very worn M_{3-4}
PM 34482, left ramus with I_1, probably P_4 in crypt
PM 34483, juvenile edentulous left ramus
PM 34484, maxillary fragment with P^4 (inverted in crypt)

Trench 4, Unit 1, top 1 foot
TMM 41106-497, left M_2
TMM 41106-540, left maxillary fragment with M^{1-2}, part of M^3
TMM 41106-541, left ramus with P_4–M_4
TMM 41106-570, left dP_4
TMM 41106-577, left M^1
TMM 41106-5131, left dP_4
TMM 41106-5132, right M^1
TMM 41106-5133, right M^2
TMM 41106-5134, right dP_4
TMM 41106-5135, anterior ⅔ left M^1
TMM 41106-5136, broken left P^4
TMM 41106-5137, left M^1
TMM 41106-5138, right P^4
TMM 41106-5139, left P_3
TMM 41106-5140, left P^3
PM 34485, right ramus fragment with P_4–M_1
PM 34486, left ramus fragment with I_1, P_3, dP_4
PM 34487, left ramus fragment with I_1
PM 34488, right maxillary fragment with broken M^{2-3}
PM 34489, left P_3

Trench 4, Unit 2, Level 1
TMM 41106-314, right maxillary with P^3, dP^4, M^1, part of M^2
WAM 75.1.135, left maxillary fragment with M^{1-2}
WAM 75.1.136, right ramus fragment with M_{2-3}
PM 34490, left P_3
PM 34491, worn right P_4
PM 34492, right M^1
PM 34493, right M^2
PM 34494, right M_2
PM 34495, right M_1
PM 34496, left M_1
PM 34497, right M^2
PM 34498, right M^3
PM 34499, left M_1
PM 34500, right M^1
PM 34501, left M^2

PM 34502, left M^1
PM 34503, left M_2
PM 34504, left M^1, M^2, or M^3
PM 34505, right M_2
PM 34506, anterior ⅔ left M^2 or M^3
PM 34507, right M^2
PM 34508, left M^3
PM 34509, edentulous left ramus
PM 34511, right maxillary fragment with M^2
PM 36873, posterior ½ lower molar
PM 36874, right ramus fragment with M_{2-3}
PM 36875, left maxillary fragment with dP^4, P^4, and M^2 in crypts, alveoli for P^3, M^1 (fig. 4A)
PM 36876, right maxillary fragment with M^{1-2}

Trench 4, Unit 2, Level 2
TMM 41106-12, left maxillary with P^3, crypt for P^4
PM 36880, ¾ right M_2
PM 36881, left M^3 or M^2
PM 36882, left M^2
PM 36883, left M^3
PM 36884, 36885, two left M^1s
PM 36886, right M_2 or M_3
PM 36887, left M_3
PM 36888, left ramus fragment with dP_4
PM 36889, edentulous right ramus fragment
PM 36890, edentulous left ramus fragment
PM 36891, edentulous left maxillary fragment
PM 36892, left maxillary fragment with M^1
PM 36893, left maxillary fragment with broken P^4, M^1
PM 36895, left dP_4
PM 36896, right dP_4
PM 36897, left P_4
PM 36898, posterior ⅞ right P_4
PM 36899, posterior ½ left P_4
PM 36900, left M_1
PM 36901, left P^3
PM 36902, left P^3 (uncertain since tooth is broader than rest of sample, blade is not compressed, and has labial groove)
PM 36903, left M_1 (has peculiar uninterrupted protoconid ridge anteriorly)
PM 38712, left M_2

Trench 4, Unit 2, Level 3
TMM 41106-2, right ramus fragment with M_{1-2}

Trench 4, Unit 4
TMM 41106-63, right maxillary with P^3, dP^4, M^1

Trench 4, Units 4–5
WAM 75.1.149, 150, two right P^4s
WAM 78.3.1, 3, two left dP_4s
WAM 78.3.2, right dP_4
PM 36904, right P_4
PM 36905, right P^4
PM 36906–36909, four left dP_4s
PM 36910–36912, three right dP_4s
PM 36913, right P_4
PM 36914, left P_4
PM 36915–36918, four right P_4s
PM 36919, right P^4
PM 36920, left P_4
PM 36921, left dP_4
PM 36922, 36923, two right M_1s
PM 36924, right M^1 or M^2
PM 36925–36929, five right dP^4s

PM 36930, 36931, two left dP^4s
PM 36932–36934, three left P_3s
PM 36935–36938, four right P_3s
PM 36939–36942, four left P^3s
PM 36943–36948, six right P^3s
PM 36949–36951, three right M_1s
PM 36952, right M^3
PM 36954–36956, three right M^1s or M^2s
PM 36957, left M_2
PM 36958, left M_1
PM 36959–36962, four right M^3s
PM 36963–36965, three right M^1s
PM 36966, left M^3
PM 36967, right M^2
PM 36968, 36969, two left I_1s
PM 36970, molar fragment
PM 36971, left M_1
PM 36972, left I_1
PM 36973, right dP_4
PM 36974, 36975, two molar fragments
PM 36976, left I_1
PM 36977, right M_1
PM 36978, right dP_4
PM 36979, 36980, two molar fragments

Trench 4, Unit 7, Level 1
WAM 78.3.4, right M_2
WAM 78.3.5, left M_2
WAM 78.3.6, left M^1
WAM 78.3.7, right M_2
WAM 78.3.8, right M^2 or M^3
PM 36989, 36990, two left P_4s
PM 36991, 36992, two right P^4s
PM 36993–36996, four I_1s
PM 36997, 36998, two right M^3s
PM 36999, 37000, two right M_2s
PM 37001, 37002, two left M_1s
PM 37703, left M_3
PM 37004, 37005, two left M^1s
PM 37006, left M^2 or M^3
PM 37007, right M_1
PM 37008, 37009, two left M_2s
PM 37010, 37011, two right M^2s or M^3s
PM 37012, left dP^4
PM 37013, left P^3
PM 37014, left M_1
PM 37015, left M_2 or M_3
PM 37016, right ramus fragment with M_3, alveoli for M_2, M_4

Trench 4, Unit 7, Level 2
PM 37017, left maxillary fragment with M^1
PM 37018, right P^4
PM 37019, 37020, two ramus fragments
PM 37021, left ramus fragment with broken molar, probably M_2
PM 37022, 37023, two left P^3s
PM 37024–37026, three right P_3s
PM 37027–37029, three left P_3s
PM 37030, 37031, two right P^3s
PM 37032, 37033, two right P_3s
PM 37034–37037, four broken left P^4s
PM 37038, 37039, two broken right P_4s
PM 37040, left P_3

PM 37041, left P^3
PM 37042, 37043, two left dP^4s
PM 37044, left P_4
PM 37045, right P_4
PM 37046, 37047, two right dP_4s
PM 37048, left dP_4
PM 37049–37057, nine I_1s
PM 37058–37060, three right M_2s
PM 38617, 38618, two right M_2s
PM 38619–38623, five left M^1s
PM 38624, left M^2
PM 38625–38627, three left M_2s or M_3s
PM 38628–38631, four right M_1s
PM 38632–38635, four right M^3s
PM 38636, left M_3
PM 38637–38639, three right M^1s
PM 38640, right M_1
PM 38641, right M_3 or M_2
PM 38642, left M_2
PM 38643, 38644, two left M_1s
PM 38646, 38647, two left M_4s
PM 38648, right M_1
PM 38649, left M_1
PM 38650, broken tooth

Trench 5, Unit 6
TMM 41106-589, left P^3
TMM 41106-593, left P_4
TMM 41106-598, right P^4
TMM 41106-630–633, three left dP^4s
TMM 41106-634, left lower molar fragment
TMM 41106-635, right dP^4
TMM 41106-637, left M_1 or M_2
TMM 41106-638, left dP^4
TMM 41106-639, left lower molar
TMM 41106-642, left dP_4
TMM 41106-645, right M_1 or M_2
TMM 41106-646, right dP_4
TMM 41106-5028, left P^4
TMM 41106-5109, right P^4
TMM 41106-5111–5115, five right P_3s
TMM 41106-5116, right P^3
TMM 41106-5118, -5119, two left P^3s
PM 38651, 38652, two left M^2s
PM 38653, broken M_3 or M_2
PM 38654, right M^3 or M^2
PM 38655–38658, four left M^1s
PM 38659, broken left M^2
PM 38660–38663, four left M^3s or M^2s
PM 38664–38666, three right M^1s
PM 38667, 38668, two right M^2s
PM 38669, left M_2 or M_3
PM 38670, right M_2 or M_1
PM 38671, left M_1 or M_2
PM 38672, left M^3
PM 38678–38685, eight right lower incisors
PM 38686, right M_2

Trench ?, Unit ?; probably Trench 3, Unit 3
WAM 75.1.148, right ramus fragment with P_3, dP_4

Trench ?, Unit ?, Level ?
TMM 41106-5141, right M_1 or M_2

Comparative Material

Webb's Cave
PM 36894, right ramus with P_4, broken M_{1-4}

Description

Skull.—Several maxillary fragments show some morphological characters which permit comparison with the skulls of various rat-kangaroos. Since most of these fragments are from juvenile individuals, we have used juveniles for comparison where they were available. The anterior opening of the postorbital canal lies approximately over the midpoint of P^3, usually as a simple opening. In one specimen (TMM 41106-34) this foramen opens into a broad, deep depression on the side of the maxillary. Within the central part of this depression there is a flat arching strut of bone that forms a tunnel about one-fourth the diameter of the infraorbital foramen, large enough to pass a sizable branch(es) of the infraorbital nerve or artery (fig. 4B). This character apparently is variable in potoroines; a specimen of *Bettongia lesueur* from Koomooloobooka Cave (TMM 41230-108) shows this "bifurcated" condition only on one side of the skull. The posterior opening of the infraorbital canal lies close to the sphenopalatine foramen, as it does in *Bettongia;* it differs in this character from *Potorous tridactylus* (PM 6706 and TMM M-2549). Behind and slightly lateral to the posterior opening of the infraorbital canal are two or three small nutrient foramina which extend downward into the alveoli of the teeth. One branch of the infraorbital canal extends downward and anteriorly and emerges as a small foramen on the palate just anterior to the P^3. At least one lacrimal foramen is present. The canal leading downward and anteriorly from it can be seen on the inside of the maxillary (fig. 4B). This foramen probably is equivalent to the inferior lacrimal foramen described by Stirton (1963) for *Protemnodon,* which is present in most, if not all, macropodids.

Upper Dentition.—No incisors have been found among the Madura Cave materials which can definitely be associated with skull fragments identified as *Caloprymnus.* One edentulous premaxillary (PM 34434; fig. 4H) has been tentatively referred to this genus on the basis of alveolar dimensions and positions, but this specimen also might belong to *Lagorchestes,* whose premaxillary is very similar to that of *Caloprymnus.*

The P^3 is a laterally compressed, serrate blade, with three strong grooves followed by one weak groove dividing the crown labially and lingually into

---

Opposite:

FIG. 4. *Caloprymnus campestris* from Madura Cave. **A,** PM 36875. Left maxillary of a juvenile with dP^4, P^4, and M^2 in their crypts, alveoli of P^3 and M^1, shown in ventral and labial views. **B,** TMM 41106-34. Left maxillary of a juvenile with P^3, P^4 removed from crypt, M^{1-2}, shown in lingual (left), ventral, and labial views. **C,** TMM 41106-167. Left maxillary of a juvenile with P^3, dP^4, M^{1-2}, alveoli for M^3, shown in labial (left), ventral, and lingual views. **D,** TMM 41106-310. Right maxillary fragment of an adult with P^4, M^1, shown in labial and crown views. **E,** TMM 41106-358. Right maxillary fragment of an adult with M^{2-3}, shown in crown and lingual views. **F,** TMM 41106-307. Left maxillary fragment of an adult with M^{1-3}, shown in crown and lingual views. **G,** TMM 41106-309. Right maxillary fragment of an adult with M^{3-4}, shown in crown and lingual views. **H,** PM 34434. *Incertae sedis,* probably *C. campestris,* possibly *Lagorchestes.* Edentulous right premaxillary shown in labial and ventral views.

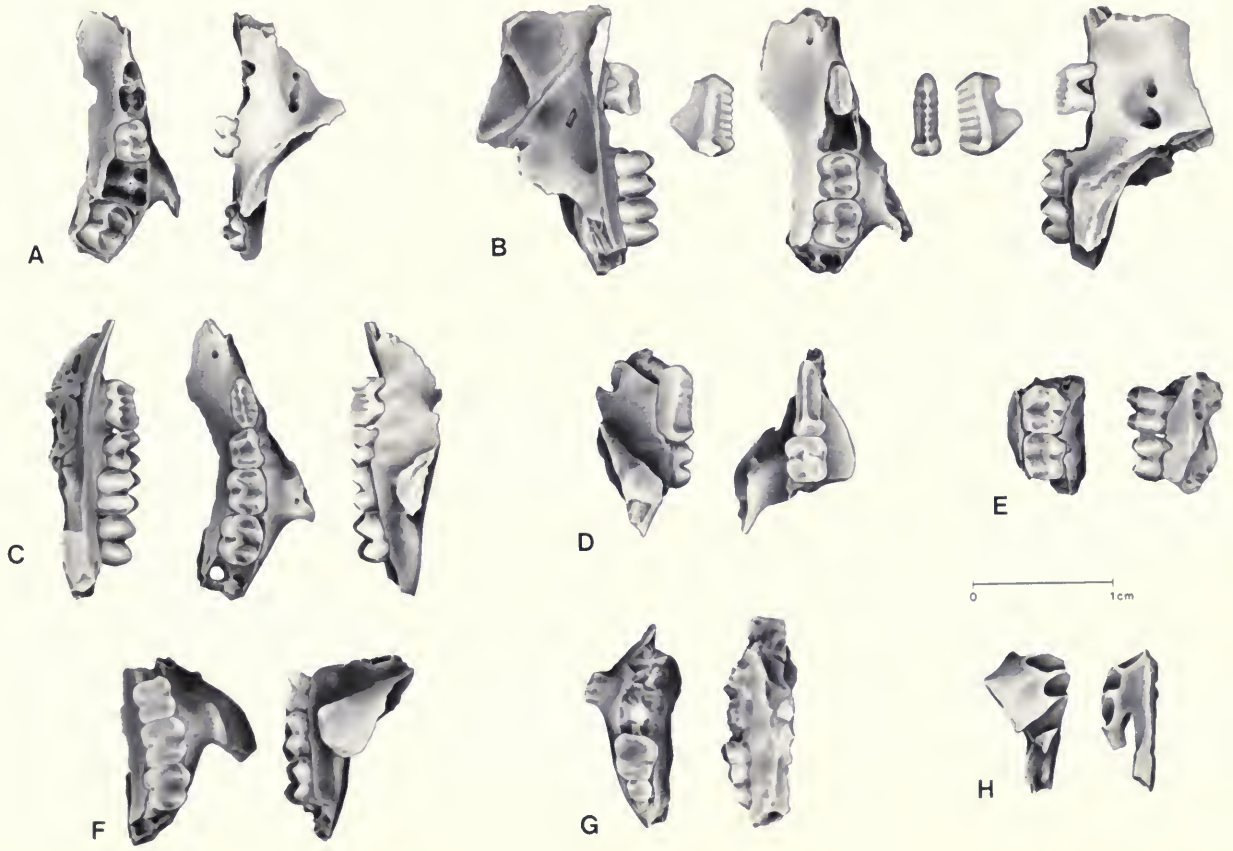
A
B
C
D
E
0
1cm
F
G
H

three well-defined anterior cusps and two less well-defined posterior cusps. The combined length of the posterior pair of cusps is two to two and one-half times that of either of the preceding cusps. The two posterior cusps are strongly compressed laterally and are aligned with the long axis of the tooth. The crest of the blade is almost straight. The tooth has three roots, one anterior and two posterior. The posterior roots lie side by side and diverge upward. A small fourth root is fused to the lingual side of the anterior root in two specimens (TMM 41106-167, 41106-359). The lingual and labial edges of the tooth have cingular shelves which are widest over the posterior roots. The shelves bear two to four (most often three) broad, low cusps which are located opposite the ridges on the sides of the blade, but are not always joined to them. Both sides of the tooth usually have the same number of cingular cusps.

The dP^4 is a rectangular tooth with four major equal-sized cusps (fig. 4A,C). A laterally compressed parastyle, indistinctly set off from the paracone, forms a short blade which is aligned with the blade of P^3. Crests extending posteriorly from the protocone and anteriorly from the hypocone join near the midline of the tooth to form a V-shaped lingual boundary for the central basin. Very weak crests extend from the apices of the paracone and metacone toward the center of the tooth but they do not join, thus leaving the labial side of the basin open. The posterior crests of the metacone and hypocone join to form a narrow posterior cingular basin. The protocone lacks an anterior crest. The anterior cingular area consists of a concave surface which slopes rootward from the parastyle to a point about halfway across the anterior face of the protocone. There is a very weak procingular ridge.

The protoloph is straight, with its lowest point close to the protocone. The metaloph has a slight sigmoid curve, with its lowest point close to the hypocone. As in Recent material from South Australia (Finlayson, 1932), the paracone and metacone contribute more to the lophs than do the protocone and hypocone. The posterior face of the metaloph has a broad convexity extending from the midpoint of the crest to the posterior cingular basin. The anterior face of the metaloph and both faces of the protoloph are flat.

A spur running anterolabially from the hypocone into the central valley was described by Finlayson (1932) in Recent specimens of *Caloprymnus campestris* from South Australia and by Tedford (1967) in a tentatively referred specimen from Lake Menindee, New South Wales. The only sign of this spur on the Madura Cave specimens is a faint bulge in that position on some specimens.

The P^4 is a straight, serrate, laterally compressed blade with no arch to the edge (fig. 4B,D). Six grooves divide the crown into seven laterally compressed cusps. The anterior six cusps are approximately the same size. The posterior cusp is approximately twice as long as any other cusp and has a broad ridge on its lingual face which extends to the valley which separates this cusp from the posterointernal cuspule. The posterointernal cuspule is conical when unworn and is about half the height of the posterior cusp of the blade. A lingual cingulum is present which bears three to five low, rounded cuspules which are located opposite the grooves in the blade and are joined to the cusps of the blade by weak ridges. The anterior cusp of the blade has a well-defined anterior ridge.

The general pattern of M^1, M^2, and M^3 (fig. 4A–G) is similar to that of dP^4. There is no parastyle, but anterior crests of the protocone and paracone join to form a prominent ridged procingulum and an anterior cingular basin. The posterior crest of the protocone and the anterior crest of the hypocone are

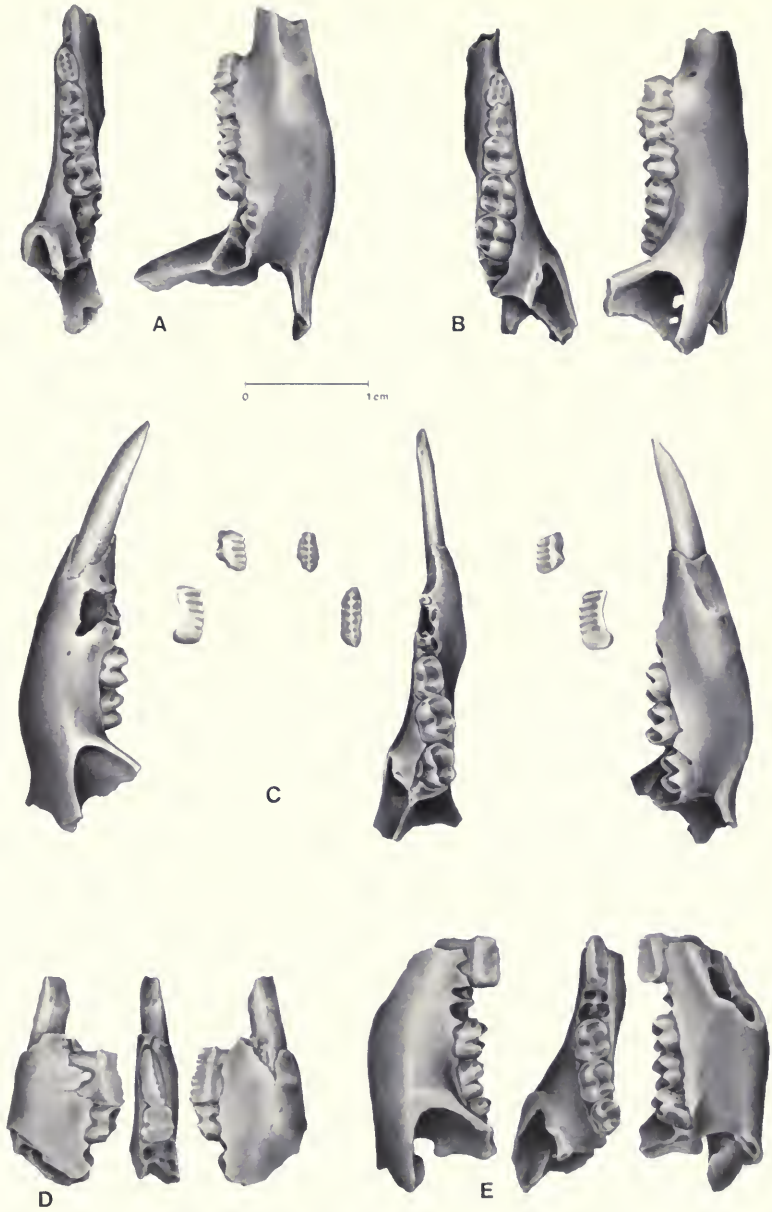

FIG. 5. *Caloprymnus campestris* from Madura Cave. **A,** TMM 41106-160. Left mandible of a juvenile with P_3, dP_4, M_{1-2}, alveolus for M_3, crypt for M_4, shown in dorsal and lingual views. **B,** TMM 41106-161. Right mandible of a juvenile with P_3, dP_4, M_{1-3}, alveoli for M_4, shown in dorsal and labial views. **C,** TMM 41106-163. Left mandible of a juvenile with I, P_3, P_4 (all removed), M_{1-2}, M_3 in crypt, crypt for M_4, shown in labial (left), crown, and lingual views. **D,** TMM 41106-164. Left ramus fragment of an adult with broken incisor and very worn P_4 and M_1, shown in labial (left), crown, and lingual views. **E,** TMM 41106-166. Left ramus fragment of an adult with P_4, M_{2-4}, alveolus for M_1, shown in labial (left), crown, and lingual views.

TABLE 5. Position of anterior end of masseteric canal in specimens of *Caloprymnus campestris* of various dental ages.

Dental stage	Specimen No.	Eruption stage	Position of anterior end of masseteric canal
1	TMM 41106-354	dP_4 in place, M_1 erupting	Posterior to M_1
2	TMM 41106-351	M_1 in place, M_2 erupting, M_3 unerupted	Anterior end of M_2
3	TMM 41106-346	P_3, dP_4, M_1* in place, M_2 erupting*	Posterior end of M_1
3	TMM 41106-349	dP_4–M_1* in place, M_2 erupting	Posterior end of M_1 alveolus
3	TMM 41106-352	dP_4, M_1 in place, M_2 erupting*	Posterior end of M_1
4	TMM 41106-353	P_3,* dP_4,* M_1,* M_2 erupting	Midpoint of M_1 alveolus
5	TMM 41106-2	M_1, M_2 in place, M_3 erupting?	Protolophid of M_1
5	TMM 41106-344	P_3–M_2 in place, M_3 erupting*	Hypolophid of M_1
5+	TMM 41106-345	P_3–M_2 in place, M_3 unerupted	Posterior end of M_1
6	PM 36894 (Webb's Cave)	P_4–M_4 in place	Anterior end of M_1

* Based on condition of alveoli.

directed labially and meet in the central valley in either a V or a U. The posterior crest of the paracone and the anterior crest of the metacone are weakly developed. They extend from the apices of the cusps toward the central valley and then turn lingually in varying ways. In some specimens the crests almost reach the central valley and then turn sharply lingually, while in other specimens the crests swing lingually in a smooth curve about halfway to the bottom of the central valley. In some specimens the posterior crest of the paracone bifurcates and one ridge is directed lingually, while the other, which usually is more rounded, remains near the labial edge of the cusp, disappearing near the bottom of the median valley. The labial crests usually do not join in the central valley as do the lingual crests. The posterior crests of the metacone and hypocone join to form a well-developed postcingulum with a deep posterior cingular basin.

The protoloph and metaloph are slightly wavy. They join the paracone and metacone at their apices, but join the protocone and hypocone on their labial sides below their apices. The protoloph joins the side of the protocone slightly anterior to its apex; the metaloph joins the side of the hypocone slightly posterior to its apex. The protoloph has a low rounded bulge on its anterior face. The metaloph has a similar, but larger, bulge on its posterior face; this posterior bulge may be ridged. The faces of both metaloph and protoloph which border on the central valley are flat.

The anterolabially directed spur from the hypocone mentioned by Finlayson (1932) and Tedford (1967) is variable in its expression. An enamel column may be present between the protocone and hypocone of M^1. The cusps and ridges of all of these molars are higher and sharper than those of *Bettongia*.

The only M^4 in the Madura Cave collection (TMM 41106-309; fig. 4G) is so heavily worn that few features can be discerned. It is markedly smaller than M^3, and the posterior end is reduced so that the tooth has a triangular shape.

TABLE 6. Measurements of upper dentitions of *Caloprymnus campestris* from Unit 1 of Madura Cave.

		TMM 41106-540	PM 34488	TMM 41106-570	TM 41106-5140	TM 4106-5138
P^3	L	...	...	...	3.30	...
	AW	...	...	...	1.25	...
	PW	...	...	...	1.22	...
	Max. W	...	...	...	1.71	...
dP^4	L	...	...	2.89	...	...
	AW	...	...	2.20	...	...
	PW	...	...	2.43	...	...
P^4	L	...	...	...	...	5.85
	AW	...	...	...	...	1.78
	PW	...	...	...	...	1.98
M^1	L	3.04	...	...	...	...
	AW	2.96	...	...	...	...
	PW	2.93	...	...	...	...
M^2	L	3.46	...	...	...	...
	AW	3.27	...	...	...	...
	PW	3.27	...	...	...	...
M^3	L	...	3.50	...	...	...
	AW	...	2.89	...	...	...
	PW	...	2.43	...	...	...

Mandible.—The mandible is short and deep, as in *Bettongia* and unlike *Potorous*. No specimen from the Madura Cave collection has a complete ascending ramus, but the basal part is preserved in two specimens (TMM 41106-160, 41106-345; fig. 5A). The anterior edge of the ascending ramus is at a 45° angle to the tooth row, steeper than the angle found in either *Bettongia* or *Potorous*. The masseteric fossa is deep and opens anteriorly into a tunnel-like masseteric canal, which has been shown by Abbie (1939) to be confluent with the inferior dental canal and also serves as the area of insertion for the deep masseter. This canal extends to the posterior end of the alveolus for the lower incisor, which lies at the level of the posterior end of M_1 in juvenile individuals and at the level of the anterior end of M_1 in adult specimens (table 5). Other genera of potoroines show some variation in the forward extent of this canal. In *Aepyprymnus* and *Potorous* it extends to the level of M_2, and in *Bettongia*, to the middle of M_1 (Abbie, 1939). Thus, *Caloprymnus* shows as specialized a state of this character as any of the other potoroines.

The mental foramen is high on the labial side of the mandible just ahead of P_4 or P_3. All mandibles have a shallow pit on the labial side just below M_1. In some specimens this pit is elongated, somewhat like the labial groove in *Protemnodon* (Stirton, 1963, p. 123). There is an equidimensional concave-upward pterygoid fossa. The mandibular foramen is located at the anterior end of this fossa directly under the posterior end of the tooth row. The symphysis is not ankylosed. The symphyseal areas are prominent and roughly oval with an irregular surface. The posterior end of the symphysis lies under dP_4 in juvenile individuals and under P_4 in adult individuals. There is a large pit immediately posterior to the symphysis.

Lower Dentition.—The lower incisor is long, gently tapered, and weakly curved, with a suboval cross section except for a flattening on the ventral edge of the

TABLE 7. Statistical data on upper dentitions of *Caloprymnus campestris* from Units 2 to 4–5 of Madura Cave.

		N	Mean ± SE	SD	CV (%)	OR
P^3	L	24	3.61 ± .049	.24	6.65	3.09–3.95
	AW	24	1.31 ± .022	.11	8.40	1.14–1.52
	PW	24	1.28 ± .033	.16	12.50	1.14–1.90
	Max. W	24	1.85 ± .039	.19	10.27	1.43–2.20
dP^4	L	21	2.93 ± .035	.16	5.46	2.58–3.19
	AW	21	2.14 ± .031	.14	6.54	1.97–2.43
	PW	21	2.43 ± .037	.17	7.00	2.05–2.66
P^4	L	6	5.53	...	...	5.32–5.78
	AW	6	1.64	...	...	1.44–2.05
	PW	7	2.05	...	...	1.86–2.28
M^1	L	16	3.26 ± .035	.14	4.29	3.04–3.50
	AW	17	2.90 ± .046	.19	6.55	2.66–3.30
	PW	16	2.84 ± .025	.10	3.52	2.74–3.12
M^2	L	16	3.43 ± .045	.18	5.25	3.12–3.72
	AW	16	3.17 ± .040	.16	5.05	2.96–3.50
	PW	14	2.97 ± .035	.13	4.38	2.81–3.34
M^3	L	4	3.28	...	...	3.19–3.42
	AW	4	3.12	...	...	2.96–3.19
	PW	3	2.63	...	...	2.48–2.66
M^4	L	1	2.36	...	...	...
	AW	1	1.78	...	...	...
	PW	...	...	...	...	...

medial surface (fig. 5C). It shows somewhat greater lateral compression distally than proximally. The ventral and lateral surfaces of the crown are covered with enamel, except for the most proximal quarter of the lateral surface. The medial surface has a fairly even enamel band along its ventral edge which gradually thins to nothing in the most proximal quarter of the crown. The rest of the medial surface and all of the dorsal surface except for its extreme lateral edge lack enamel. Most of the lower incisors from the lower units in the cave have enamel extending slightly higher on the medial side.

The P_3 is a serrate, bladelike tooth with three grooves which divide it into four laterally compressed cusps. The anterior and posterior cusps are larger than the two central cusps. The posterior cusp, which is the largest, is weakly subdivided on both sides and across the ridge by a shallow groove. This groove usually is removed by wear. The posterior half of this cusp is turned lingually, and considerably overhangs the posterior roots of the tooth. The labial side of the tooth has a prominent bulge centered over the posterolabial root. This bulge shows subdued extensions of the grooves that divide the crown. The lingual side of the tooth has a low, rounded cingulum which extends from the anterior part of the posterior cusp to the posterior part of the anterior cusp. This cingulum bears two low, blunt cusps which lie opposite the two central cusps of the blade. The labially expanded base of the crown shows some variation at its posterior end. In TMM 41106-160 and 41106-161 its edge is a smooth arc. In TMM 41106-344 the edge is sharply constricted at its posterior end. TMM 41106-163 is less sharply constricted. Like P^3, P_3 has one anterior root and two side-by-side posterior roots (fig. 5A,B).

The dP_4 is a subtriangular tooth with one anterior root and two posterior

TABLE 8. Statistical data on upper dentitions of *Caloprymnus campestris* from Unit 7 of Madura Cave.

		N	Mean ± SE	SD	CV (%)	OR
P^3	L	10	3.55 ± .060	.19	5.35	3.27–3.84
	AW	10	1.23 ± .002	.08	6.50	1.14–1.37
	PW	10	1.33 ± .002	.08	6.02	1.22–1.44
	Max. W	10	1.75 ± .051	.16	9.14	1.44–1.82
dP^4	L	8	3.02 ± .049	.14	4.64	2.81–3.19
	AW	8	2.28 ± .078	.22	9.65	1.90–2.66
	PW	8	2.45 ± .078	.22	8.98	2.20–2.88
P^4	L	3	5.23	...	...	4.98–5.55
	AW	2	1.45	...	...	2.37–1.52
	PW	2	1.64	...	...	1.60–1.67
M^1	L	1	3.50	...	...	...
	AW	1	3.04	...	...	...
	PW	1	2.92	...	...	...

roots. The anterior end of the tooth is laterally compressed all the way to the base of the crown. The blade thus formed has its anterior half oriented parallel to the long axis of the tooth and its posterior half turned lingually at an angle of about 45° to the long axis of the tooth. The change in orientation between the two halves is abrupt. In some specimens the blade is weakly divided into two cusps by a shallow groove. At the point of inflection there is a ridge on the labial side of the blade which extends rootward and posteriorly to join the anterior crest of the hypoconid, forming the labial boundary of the central basin well in from the labial edge of the tooth. The lingual border of the central basin is formed by the merging of the bases of the lingual cusps. In many specimens this border is enhanced by the joining of crests extended from the lingual cusps. The hypoconid and entoconid are subequal in size when unworn and are joined by a sharp ridge. The crest of the entoconid makes the greatest contribution to this ridge. Crests extend posteriorly from the apices of the hypoconid and entoconid to surround a broad posterior basin.

The P_4 is a relatively low-crowned, serrate, bladelike tooth with two roots (fig. 5C–E). In profile its cutting edge is almost straight rather than being slightly arched as it is in *Bettongia*. In crown view the crest bends lingually in a gentle arc which is most pronounced in the posterior half of the blade. Five well-developed pairs of grooves divide the tooth into six cusps. The anterior cusp may be larger than the next four cusps. The posterior cusp is two to three times the size of any of the four preceding cusps. It is strongly compressed laterally and is inflected lingually at an angle of about 40° to the long axis of the tooth. The lingual surface of the tooth has a cingular bulge which is variably subdivided by extensions of the grooves on the blade. The labial surface of the tooth is almost flat, but may have a similar, though smaller, cingular bulge.

The M_1, M_2, and M_3 are rectangular teeth with four nearly equal-sized cusps (fig. 5A–E). The anterior moiety of M_1 is slightly narrower than the posterior moiety (tables 9, 10). The protolophid and the hypolophid are well developed. These lophids are sharp when unworn and are much higher than those of *Bettongia*. The lophids join the lingual conids at their apices and slope down from there to the midline of the tooth. As pointed out by Finlayson (1932) for the Recent population from South Australia, the metaconid and entoconid contribute more to the lophids than do the protoconid and hypoconid. The hy-

TABLE 9. Measurements of lower dentitions of *Caloprymnus campestris* from Unit 1 of Madura Cave.

		TMM 41106-541	PM 34485	PM 34486	PM 34489	TMM 41106-5131	TMM 41106-5134	TMM 41106-5139	Mean
P_3	L	...	...	...	3.27	...	...	3.04	3.16
	AW	...	...	...	1.14	...	...	1.22	1.18
	PW	...	...	1.37	1.06	...	...	.99	1.14
	Max. W	...	...	1.75	1.82	...	...	1.90	1.82
dP_4	L	...	...	2.81	...	2.81	2.96	...	2.86
	AW	...	...	1.98	...	1.75	1.56	...	1.76
	PW	...	...	2.05	...	2.32	2.05	...	2.14
P_4	L	4.94	...	...	...	...	...	...	4.94
	AW	1.75	...	...	...	...	...	...	1.75
	PW	1.67	1.52	...	...	...	...	...	1.60
M_1	L	2.81	2.96	...	...	...	...	...	2.89
	AW	2.13	...	...	...	...	...	...	...
	PW	2.51	...	...	...	...	...	...	...
M_2	L	3.08	...	...	...	...	...	...	...
	AW	2.74	...	...	...	...	...	...	...
	PW	2.74	...	...	...	...	...	...	...
M_3	L	3.12	...	...	...	...	...	...	...
	AW	2.96	...	...	...	...	...	...	...
	PW	2.74	...	...	...	...	...	...	...
M_4	L	2.74	...	...	...	...	...	...	...
	AW	2.81	...	...	...	...	...	...	...
	PW	2.05	...	...	...	...	...	...	...
M_{1-3}	L	8.97	...	...	...	...	...	...	...
M_{1-4}	L	11.67	...	...	...	...	...	...	...

polophid is straight. The protolophid is slightly convex anteriorly. In unworn teeth prominent crests extend downward and lingually from the apices of the protoconid and hypoconid toward the midline of the tooth and join in the central valley to form the labial boundary of the central basin. The metaconid and entoconid have weakly developed crests which extend down the cusps to meet at the midline of the tooth. These crests form the lingual boundary of the central basin. The procingulum of M_1 is variable. In some specimens it is only half the width of the tooth, lacks a well-defined basin, and is joined by a ridge only to the metaconid. In most specimens it is larger, occupying up to three-quarters of the width of the tooth, has a definite basin, and is joined by ridges to both the metaconid and the protoconid. A few specimens have procingular basins, but lack the ridge from the protoconid. The M_2, M_3, and M_4 all have procingula which are connected to the protoconid by prominent crests and which have well-defined basins. In all specimens which are not extremely worn, the procingulum is joined to the base of the anterolabial corner of the protoconid. The posterior crests of the hypoconid and entoconid of M_{1-3} swing downward and toward the midline of the tooth, joining to form a well-defined postcingulum with a well-developed basin.

The M_4 is markedly narrower posteriorly than the other molars (fig. 5E). The

TABLE 10. Statistical data on lower dentitions of *Caloprymnus campestris* from Units 2 to 4–5 of Madura Cave.

		N	Mean ± SE	SD	CV (%)	OR
P_3	L	14	3.05 ± .040	.15	4.92	2.85–3.34
	AW	14	1.26 ± .027	.10	7.94	1.06–1.44
	PW	14	1.27 ± .032	.12	9.45	1.06–1.44
	Max. W	14	1.83 ± .021	.08	4.37	1.67–1.98
dP_4	L	19	2.74 ± .028	.12	4.38	2.51–2.96
	AW	19	1.51 ± .044	.19	12.58	1.37–1.90
	PW	18	2.00 ± .028	.12	6.00	1.82–2.36
P_4	L	11	4.80 ± .108	.36	7.50	4.26–5.40
	AW	9	1.47 ± .070	.21	14.74	1.22–1.75
	PW	11	1.57 ± .060	.20	12.74	1.22–1.82
M_1	L	12	3.17 ± .052	.18	5.68	2.89–3.60
	AW	12	2.29 ± .029	.10	4.37	2.12–2.47
	PW	13	2.64 ± .078	.27	10.22	2.36–3.43
M_2	L	15	3.48 ± .036	.14	4.02	3.27–3.72
	AW	13	2.78 ± .028	.10	3.60	2.62–2.96
	PW	13	2.95 ± .036	.13	4.41	2.74–3.12

hypoconid and entoconid are well defined. The postcingulum, formed by crests from the hypoconid and entoconid, has a basin which is located partly between the hypoconid and entoconid rather than entirely posterior to them as it is in the other molars.

DISCUSSION

A comparison of measurements of teeth from various stratigraphic units shows few differences in size (tables 6–11). The lengths of the P_4 and M_2 of two specimens from Unit 1 are below the lower limit of those teeth of the sample from Units 2 to 4–5, but larger samples would be needed to demonstrate significant differences. Comparisons of samples from Units 2 to 4–5 and Unit 7 reveal minor differences, but *t* tests give nonsignificant results ($P > .05$) in every case.

The Madura Cave specimens are smaller than the Pleistocene specimens from Lake Menindee and the Recent specimens from northeastern South Australia. A comparison of the dental measures given by Tedford (1967, p. 30) and Finlayson (1932, p. 166) shows that there is no overlap in any measurement between those samples and the sample from Madura Cave.

Caloprymnus campestris is known as a living animal only from a small area in northeastern South Australia and southwestern Queensland (Finlayson, 1932). This area has sand ridges, claypans, and gibber plains. According to Finlayson, *Caloprymnus* does not occur on the sand ridges, but seems to be restricted to the flat areas.

Caloprymnus is known from late Pleistocene and Holocene deposits at Lake Menindee, western New South Wales (Tedford, 1967) and various caves on the Nullarbor Plain (Lundelius, 1963; Archer, 1972, 1974). The time of its disappearance from the Nullarbor Plain is not known precisely, but was certainly Holocene. Its presence in surficial deposits in Webb's Cave (Lundelius, 1957, 1963) has been taken to indicate a very recent occurrence as a living animal in this area, but C^{14} dates of 1500 ± 70 BP on charcoal (TX 1148) and 5030 ± 90

TABLE 11. Statistical data on lower dentitions of *Caloprymnus campestris* from Unit 7 of Madura Cave.

		N	Mean	OR
P_3	L	8	3.14	2.96–3.50
	AW	8	1.20	1.06–1.44
	PW	8	1.28	1.14–1.52
	Max. W	8	1.79	1.67–1.98
dP_4	L	3	2.79	2.66–2.98
	AW	3	1.37	1.29–1.44
	PW	3	1.95	1.94–1.98

BP on bone (TX 1147) from a depth of 1 to 3 inches (2 to 7 cm) in this cave throw doubt on this conclusion. In addition, on two mummified specimens of *Thylacinus cynocephalus* from two other Nullarbor caves, C^{14} dates are 3280 ± 90 BP for one and 4650 ± 104 and 4550 ± 153 BP for the other (Partridge, 1967; Lowry & Merrilees, 1969). These dates indicate that there has been little or no deposition in some of these caves for significant periods of time. This, together with the dry conditions in many of these caves, which ensure good preservation, demonstrates that caution should be used in drawing conclusions about the age of material based only on its appearance or on its position on the surface. It is possible that *Caloprymnus* survived to the time of European settlement in locally favorable areas as the report of its presence on the Bunda Plateau by Tate (1879) suggests, but as yet there is no supporting evidence from the cave deposits.

Like *Dasyuroides byrnei*, *Caloprymnus* disappeared from the Nullarbor Plain some time during the Holocene when the climate was becoming drier, but still survives in a very arid area in central Australia. The reasons for the disappearance of these two animals from the Nullarbor Plain are not known. Finlayson (1958) has suggested that *Caloprymnus campestris* is competitively inferior to *Bettongia lesueur* in arid areas because of the latter's burrowing habit. He points out that, today, *C. campestris* survives only in areas in which *B. lesueur* does not occur. If Finlayson's hypothesis is correct, then we need to account for the exception to it given by the Madura Cave and Lake Menindee records. This will be considered in the conclusion.

Caloprymnus *Incertae Sedis*

MATERIAL

Trench 3, Unit 2, Level 1
PM 34434, edentulous right premaxillary, possibly *Lagorchestes* (fig. 4H)
Trench 3, Unit 2, Level ?
PM 38718, broken molar
Trench 5, Unit 6
PM 38674–38677, four upper incisors

Bettongia

Bettongia Gray, 1837
Bettongiops Matschie, 1916

The genus *Bettongia* is represented in the Madura Cave deposits by two species, *B. lesueur* and *B. penicillata*. Specimens with diagnostic characters such as sec-

torial premolars and auditory bullae can be confidently assigned to species. Table 12 lists the diagnostic features. However, the majority of the *Bettongia* material from Madura Cave consists of isolated teeth that usually cannot be identified to species; many of these specimens are listed as *Bettongia* sp. These materials show no characters that would rule out their assignment to either *B. lesueur* or *B. penicillata* or that suggest the presence of any other species of *Bettongia*.

The M^1 and M^2 of *B. penicillata* frequently have a mesostyle (Finlayson, 1958; Tedford, 1967; Marshall, 1973). All of the Madura Cave specimens which can be assigned to *B. penicillata* on other grounds have mesostyles on dP^4, M^1, and M^2. Therefore, isolated upper molariform teeth with mesostyles have been referred to *B. penicillata*. Because some specimens of *B. penicillata* have been reported to lack a mesostyle on M^1 and M^2, isolated upper molariform teeth which lack a mesostyle cannot be assigned to either species. The situation is further complicated by the fact that, on rare occasions, a specimen of *B. lesueur* may have a trace of mesostyle on dP^4, M^1, or M^2 (an example is PM 4786, positively identified as *B. lesueur* on the basis of the form and groove count of its P^3s and P^4s).

It is difficult to identify individual dP^4s to species on the basis of standard dental measurements. Considering only teeth in jaws, which can be identified on the basis of other features, the dP^4s of *B. penicillata* are smaller on the average than those of *B. lesueur*, but the two size distributions overlap. A plot of length versus anterior width for all known dP^4s from Madura Cave (fig. 6A) illustrates the extent of this overlap. In Figure 6B the points for isolated teeth have been added to the plot from Figure 6A. Small x's indicate those isolated teeth which we considered to belong to *B. penicillata* because they are small and their crowns are simple. Small circles indicate those isolated teeth which we considered to belong to *B. lesueur* because they are larger and more bulbous and have more complex crowns. Seven teeth which did not fall into either group are indicated by dots with specimen numbers. Most of the isolated teeth fall within or near the plots of the known teeth. The fact that it is only tooth proportions, rather than other consistent morphologic features, which seem to divide the two groups makes the identifications less certain. Figure 6C shows a plot of length versus posterior width for the same specimens. Overall, the results of this plot are the same as those of Figure 6B, although the two differ in detail.

Bettongia lesueur (Quoy & Gaimard, 1824)

Hypsiprymnus lesueur Quoy and Gaimard, 1824
Hypsiprymnus graii Gould, 1840
?*Bettongia graii* Gray, 1841
Perameles harveyi Waterhouse, 1842
Bettongia lesueuri Thomas, 1888
Bettongiops lesueuri Matschie, 1916

MATERIAL

Surface pickup

TMM 41106-20, adult skull with left and right I^1, P^4-M^3, and right ramus with I, P_4-M_3 (figs. 7, 9A-C)

TMM 41106-26, left ramus with I, P_3, dP_4, P_4 in crypt, M_1, M_2, and M_3 in crypt (fig. 10A-C)

TABLE 12. Dental and cranial characteristics used to distinguish the Madura Cave *Bettongia lesueur* from *Bettongia penicillata*.

Feature	***Bettongia lesueur***	***Bettongia penicillata***
Cheek teeth rows	Do not diverge anteriorly (nearly parallel)	Diverge anteriorly
P^3	Anterior-posterior crown height even Crown outline elongate oval Tooth longer than in *B. penicillata* Cingular shelves well defined Number of labial grooves: 6 Cusps of ridge laterally compressed and attenuated Axis of tooth aligned with dP^4 and molars	Anterior crown height greater than posterior Crown outline egg shaped Tooth shorter than in *B. lesueur* Usually poorly defined cingular shelves Number of labial grooves: 5 Cusps of ridge not tightly pinched in cross section Axis of tooth angled outward anteriorly with respect to dP^4 and molars
P^4	Crown height even (anterior and posterior) Axis of tooth straight Axis of tooth aligned with molars Crown outline not narrowed at midpoint Posterior cusps small Posterointernal cusp a ridge Number of labial grooves: 9 or 10 Long: ratio $LP^4/LM^1 = > 1.80$; $LP^4/LM^2 = > 1.74$	Crown height greater anteriorly Axis of tooth bent out anteriorly Axis of tooth angled out anteriorly Crown outline narrowed at midpoint Posterior cusps large Posterointernal cusp bulbous Number of labial grooves: 7 Short: ratio $LP^4/LM^1 = \sim 1.69$; $LP^4/LM^2 = \sim 1.62$
dP^4–M^3 (presence of mesostyle)	Mesostyle usually absent from all molariform teeth	Mesostyle often present: most often on M^1, less frequently on M^2, dP^4, M^3
M^{1-4} gradient	$M^1 < M^2 > M^3 \gg M^4$	$M^1 \geq M^2 > M^3 \gg M^4$
Auditory bulla	Relatively large: length of bulla/length of $M^{1-3} = > .63$	Relatively small: length of bulla/length of $M^{1-3} = < .60$

TABLE 12. *Continued.*

Feature	*Bettongia lesueur*	*Bettongia penicillata*
P_3	Axis aligned with molariform teeth	Axis angled outward anteriorly
	Crown height even (anterior and posterior)	Crown height greater anteriorly
	Crown outline a narrow oval with slight constriction	Crown outline a rounded, bulbous oval, usually with no constriction
	Well-defined cingular shelves	Poorly defined cingular shelves
	Cusps of ridge laterally compressed (pinched) and attenuated	Cusps of ridge not tightly pinched in cross section
	Number of labial grooves: 6, sometimes 5	Number of labial grooves: 5
P_4	Tooth axis aligned with molars	Tooth axis angled outward anteriorly
	Crown height even (anterior and posterior)	Crown height greater anteriorly
	Long and narrow	Wide and short
	Number of labial grooves: 8 or 9	Number of labial grooves: 7
M_{1-4} gradient	$M_1 < M_2 > M_3 > M_4$	$M_1 \leq M_2 > M_3 > M_4$

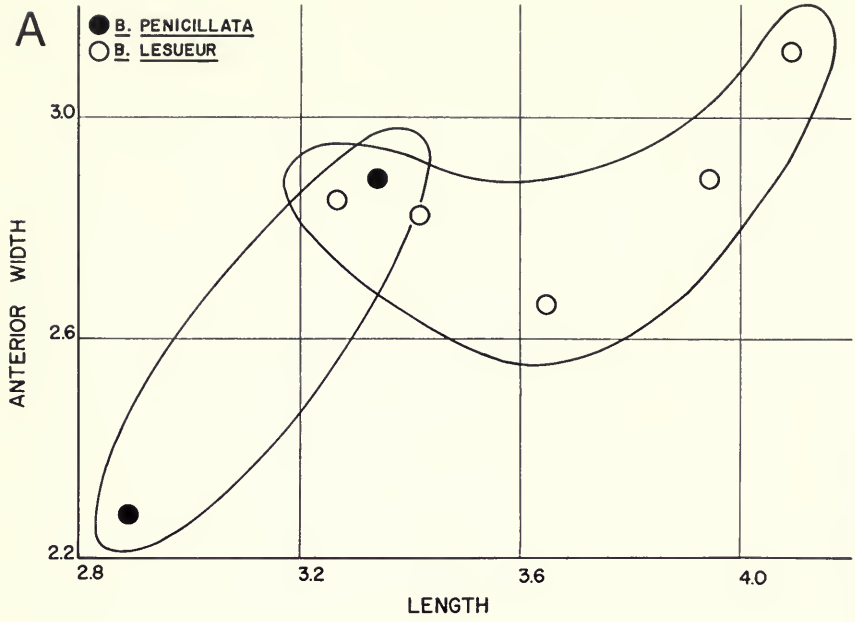
A
B. PENICILLATA
B. LESUEUR
3.0
2.6
2.2
ANTERIOR WIDTH
2.8
3.2
3.6
4.0
LENGTH

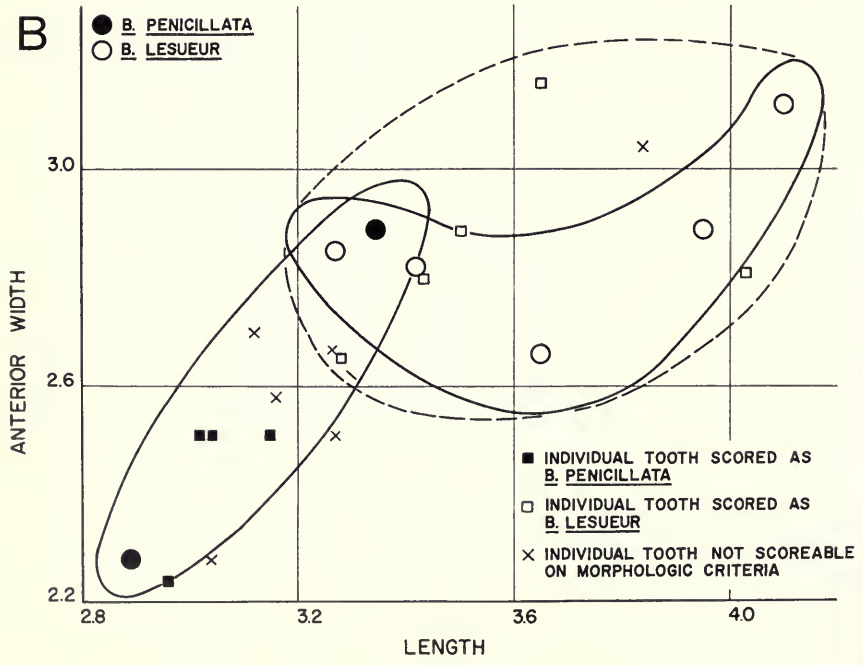
B
B. PENICILLATA
B. LESUEUR
3.0
2.6
2.2
ANTERIOR WIDTH
2.8
3.2
3.6
4.0
LENGTH
INDIVIDUAL TOOTH SCORED AS B. PENICILLATA
INDIVIDUAL TOOTH SCORED AS B. LESUEUR
INDIVIDUAL TOOTH NOT SCOREABLE ON MORPHOLOGIC CRITERIA

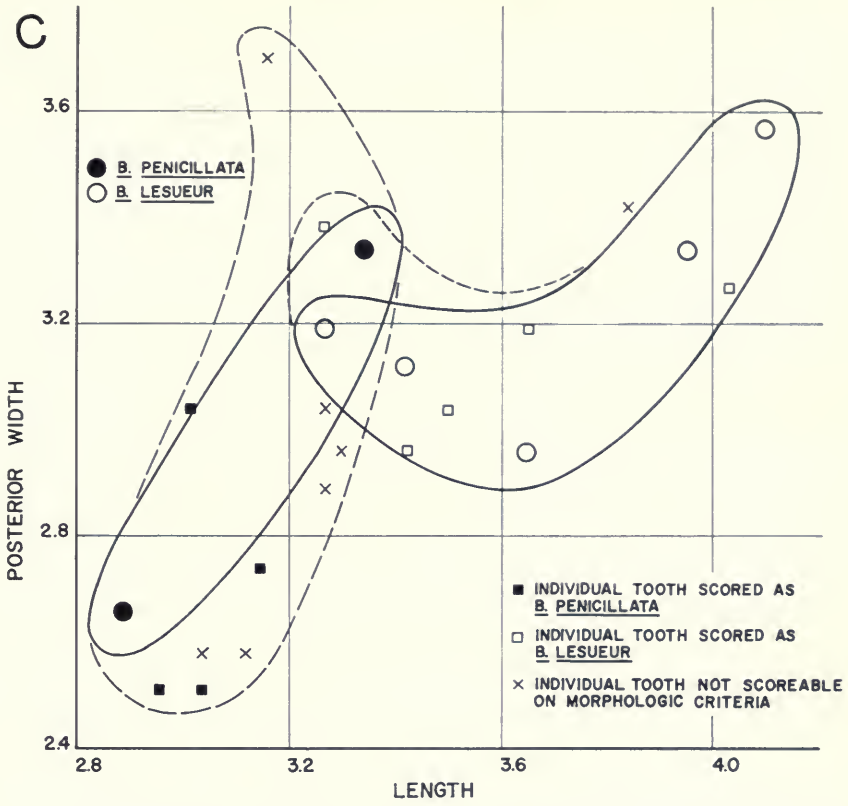

FIG. 6. Bivariate graphs of dP⁴s of *Bettongia* from Madura Cave. **A,** Plot of teeth of known specific identity. **B,** Plot of individual teeth added to **A** to show the degree of correspondence of morphological and quantitative criteria for specific assignment. The dashed line outlines the probable area of *Bettongia lesueur*. Note that, although there is an overlap zone, only one specimen is unassignable on the basis of both morphological and quantitative criteria. **C,** Plot of dP⁴s of known specific identity and of individual teeth. The dashed lines outline the probable areas of *Bettongia penicillata* and *Bettongia lesueur*. Note the area of overlap.

Trench 1, Unit 1, top 1 foot
PM 4786, right maxillary with P^3, dP^4, P^4 removed from crypt, M^{1-2}, crypt for M^3 (fig. 8A,B)
PM 4787, 4788, two right maxillaries with P^3, dP^4, P^4 exposed in crypt, M^1, crypt for M^2 (fig. 8C,D: PM 4787)
PM 4790, right ramus with I, P_3, dP_4, P_4, and M_{2-3} in crypts
PM 4791, right ramus with I, P_4 in crypt, M_2, alveoli for P_3, dP_4, and M_1
PM 4793, right ramus with I, P_3, dP_4, P_4 in crypt
PM 4795, left ramus with I, dP_4, P_4 in crypt, M_1, M_2 removed from crypt, alveolus for P_3 (fig. 9D–F)
PM 4796, left ramus with I, P_3, dP_4, P_4 in crypt, M_2, M_3 in crypt, alveolus for M_1 (fig. 10D–F)
PM 4797, left ramus with I, P_4 and M_2 in crypt, alveoli for P_3, dP_4, M_1
Trench 3, Unit 2, Level ?
TMM 41106-5, right ramus with broken I, P_4, M_{1-3}, alveoli for M_4
TMM 41106-117, left maxillary with P^4–M^2 (fig. 8E–G)
TMM 41106-118, right ramus fragment with broken I, P_4, alveolus for M_1

Trench 3, Unit 3, Level ?
TMM 41106-33, left maxillary with P^3, dP^4, M^1
PM 38727, left maxillary with broken P^4 in crypt, dP^4, M^1
Trench 4, Unit 1, Level 1–2
TMM 41106-496, right P^3
Trench 4, Unit 7, Level 1
PM 38740, 38741, two left P^3s
Trench 4, Unit 7, Level 2
PM 38645, right P_3
PM 38772, left P_3 or right P^3
Trench 5, Unit 6
TMM 41106-585, left P_4
TMM 41106-587, right P_3?
TMM 41106-588, right P^3 or left P_3
TMM 41106-5147, left P^4

Comparative Material

Koomooloobooka Cave, southwestern South Australia
TMM 41230-108
Cave N-31, southwestern South Australia
TMM 41235-31
Nannup Cave, southwestern Western Australia
PM 4998, 5141, 5144, 5146, 5150–5152, 5154, 5161–5163, 5166, 5168, 5170, 5171, 5174, 5178, 5180, 5181, 5183, 5188, 5980, 5983, 25173, 25179

Description

Skull.—The single well-preserved skull (TMM 41106-20; figs. 7A–D, 9A–C) has all the characteristic features of *B. lesueur* noted by Finlayson (1958), Marshall (1973), Tedford (1967), and Wakefield (1967). Some of these characters are summarized in Table 12. The principal characters listed by Wakefield (1967) are: (*a*) relatively short and narrow rostrum; (*b*) great inflation of auditory bullae, with bulla length approximately 25% and bulla depth below the glenoid fossa approximately 23% of the basal skull length (the values for the Madura Cave skull are 28% and 26%); (*c*) large premolars, with P^4 length approximately 14% of the basal skull length (12% in the Madura Cave skull); and (*d*) rapid decrease in size from M^1 to M^4.

Cranial, mandibular, and dental measurements of the Madura Cave material are compared in Tables 13–19 with the measurements of fossil samples from Nannup Cave, southwestern Australia, and Lake Victoria, New South Wales, and with Recent specimens from Victoria and southwestern Australia. The Madura Cave material also has been compared with measurements given by Tedford (1967, tables 5–8) for a fossil sample from Lake Menindee and Recent samples from central Australia, South Australia, southwestern Australia, and Bernier Island. Except for the dimensions of the bulla, the dimensions of the Madura Cave specimen are below the size ranges of all of these samples except for the Recent one from central Australia. The dimensions of the bulla of the Madura Cave skull are the same as or greater than the means of these dimensions for all samples except for the Recent one from South Australia, and they are within the observed ranges of that sample. The Madura Cave skull is almost as small as one from the western Northern Territory described by Finlayson (1957) as *B. penicillata anhydra* and later referred by Wakefield (1967) to *B. lesueur*.

TABLE 13. Comparison of cranial, mandibular, and dental measurements of *Bettongia lesueur* from Madura Cave with those of *Bettongia penicillata anhydra* Finlayson.

Measurement	Madura Cave TMM 41106-20	*B. penicillata anhydra**
Condylobasal length	59.3	...
Basal length	55.5	...
Greatest length	63.4	62.1†
Zygomatic breadth	39.5	37.4
Nasals, length	23.2	23.7
Nasals, greatest breadth	10.6	9.5
Interorbital constriction	13.4	12.2
Palate, length	31.3‡	32.5
Palate, inside breadth across M^2	10.3	9.4
Diastema, I^3–P^4	5.15	8.0
Incisive foramen, length	2.46	2.4
Rostrum, depth	11.6	11.6
Bulla, length	16.3	...
Bulla, maximum breadth	12.5	10.4
P^4, length	7.30	7.5
P^4, posterior width	2.43	3.0
M^{1-3}, length	11.66	10.5
P_4, length	6.08	6.4
P_4, maximum width	2.05	2.8
M_{1-3}, length	11.16	10.2
Depth of ramus to M_2	7.95	8.7
Breadth of ascending process	13.2	13.3

* Data from Finlayson, 1957. † Labeled "maximum length" by Finlayson. It is not known how this measurement was taken as the specimen is reported to lack the occiput.
‡ Estimate.

TABLE 14. Statistical data on upper dentitions of *Bettongia lesueur* from Madura Cave.

		N	OR	Mean ± SE	SD	CV (%)
P^3	L	7	4.41–5.47	4.90 ± .155	.41	8.37
	W	7	1.90–2.96	2.49 ± .132	.35	14.06
dP^4	L	5	3.27–4.10	3.68	...	...
	AW	5	2.66–3.12	2.87	...	...
	PW	4	2.69–3.57	3.27	...	...
P^4	L	3	7.30–8.73	7.84	...	...
	AW	3	2.20–2.74	2.51	...	...
	PW	3	2.43–2.89	2.63	...	...
M^1	L	7	3.80–4.56	4.02 ± .110	.29	7.21
	AW	7	3.50–4.33	3.90 ± .113	.30	7.69
	PW	7	3.80–4.71	4.04 ± .136	.36	8.91
M^2	L	3	4.18–4.86	4.46	...	...
	AW	3	4.26–4.64	4.49	...	...
	PW	3	3.95–4.41	4.23	...	...
M^3	L	1	...	3.80	...	...
	AW	1	...	3.80	...	...
	PW	1	...	3.19	...	...
M^4	L	...	...	...	...	...
	AW	...	...	...	...	...
	PW	...	...	...	...	...
M^{1-3}	L	1	...	11.66	...	...

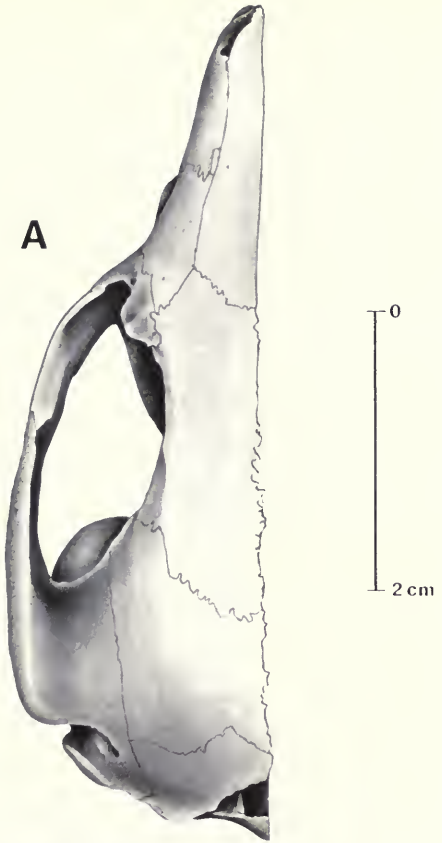
A
0
2 cm


E

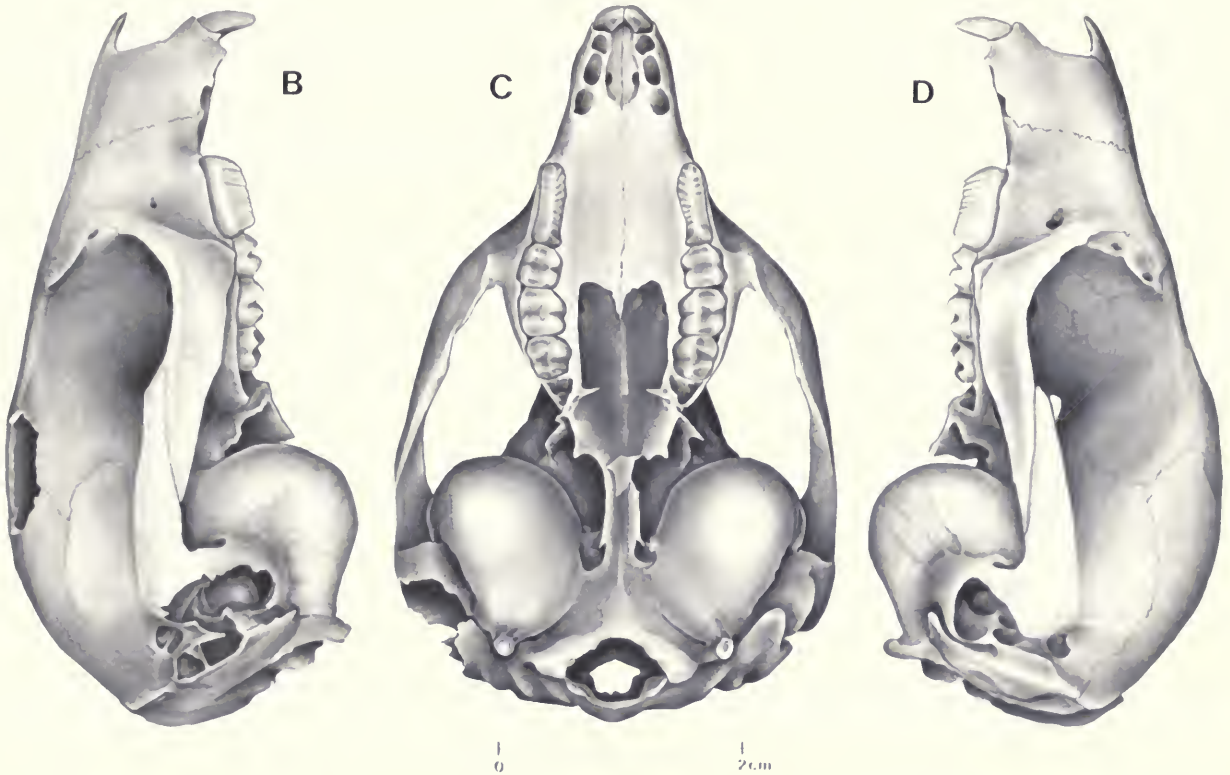

FIG. 7. *Bettongia lesueur* from Madura Cave, surface (probably Recent). TMM 41106-20, skull. **A**, Dorsal view, left half. **B**, Right lateral view. **C**, Ventral view. **D**, Left lateral view. **E**, Posterior view.

TABLE 15. Statistical data on lower dentitions of *Bettongia lesueur* from Madura Cave.

		N	OR	Mean ± SE	SD	CV (%)
P_3	L	6	3.80–4.94	4.23	...	...
	W	6	2.28–2.51	2.39	...	...
dP_4	L	5	3.50–3.72	3.60	...	...
	AW	5	1.98–2.20	2.09	...	...
	PW	5	2.54–2.93	2.77	...	...
P_4	L	3	6.08–6.84	6.49	...	...
	AW	3	2.20–2.51	2.33	...	...
	PW	3	2.05–2.66	2.36	...	...
M_1	L	4	3.65–4.10	3.88	...	...
	AW	4	3.04–3.34	3.22	...	...
	PW	4	3.27–3.72	3.53	...	...
M_2	L	8	3.88–4.56	4.14 ± .085	.24	5.80
	AW	8	3.57–4.56	3.90 ± .102	.29	7.44
	PW	8	3.57–3.95	3.70 ± .046	.13	3.51
M_3	L	3	3.57–3.65	3.62	...	...
	AW	3	3.57–3.80	3.72	...	...
	PW	3	2.96–3.42	3.24	...	...
M_4	L	...	...	...	...	...
	AW	...	...	...	...	...
	PW	...	...	...	...	...
M_{1-3}	L	1	...	11.16	...	...

TABLE 16. Statistical data on upper dentitions of *Bettongia lesueur* from Lake Victoria (data from Marshall, 1973).

		N	OR	Mean ± SE	SD	CV (%)
P^3	L	5	4.8–5.3	5.02 ± .079	.179	3.57
	W	6	2.4–2.7	2.52 ± .054	.133	5.28
dP^4	L	10	3.3–3.9	3.60 ± .061	.194	5.39
	Max. W	10	2.8–3.4	3.15 ± .065	.207	6.57
P^4	L	18	7.7–9.0	8.21 ± .097	.411	5.01
	Max. W	18	2.7–3.5	3.01 ± .062	.265	8.80
M^1	L	49	3.7–4.6	4.16 ± .031	.217	5.22
	AW	45	3.4–4.5	4.93 ± .039	.266	6.77
	PW	47	3.6–4.6	4.03 ± .034	.233	5.78
M^2	L	48	4.0–4.8	4.43 ± .029	.202	5.56
	AW	48	3.7–4.8	4.30 ± .034	.233	5.42
	PW	49	3.7–4.5	4.07 ± .028	.195	4.79
M^3	L	35	3.6–4.5	4.00 ± .035	.206	5.15
	AW	34	3.1–4.2	3.81 ± .042	.242	6.35
	PW	34	2.8–3.6	3.25 ± .039	.227	6.98
M^4	L	19	2.5–3.0	2.73 ± .044	.191	7.0
	AW	19	2.3–3.1	2.66 ± .055	.241	9.06
	PW	...	...	...	...	...
M^{1-3}	L	31	11.6–13.3	12.58 ± .093	.518	4.12

TABLE 17. Statistical data on lower dentitions of *Bettongia lesueur* from Lake Victoria (data from Marshall, 1973).

		N	OR	Mean ± SE	SD	CV (%)
P_3	L	36	3.7–4.7	4.28 ± .042	.253	5.91
	W	39	2.2–2.7	2.44 ± .025	.154	6.31
dP_4	L	41	2.9–3.8	3.37 ± .030	.195	5.79
	Max. W	40	2.6–3.1	2.77 ± .021	.135	4.87
P_4	L	48	6.1–7.6	6.80 ± .050	.346	5.09
	Max. W	53	2.2–3.0	2.49 ± .023	.165	6.63
M_1	L	98	3.5–4.2	3.92 ± .019	.192	4.90
	AW	89	3.0–3.8	3.33 ± .020	.192	5.77
	PW	91	3.2–4.2	3.68 ± .021	.200	5.43
M_2	L	87	3.8–4.8	4.42 ± .023	.214	4.84
	AW	86	3.6–4.5	4.06 ± .024	.220	5.42
	PW	84	3.3–4.5	3.95 ± .027	.245	6.20
M_3	L	68	3.8–4.6	4.09 ± .030	.147	3.59
	AW	64	3.6–4.5	3.94 ± .023	.185	4.70
	PW	62	3.2–4.3	3.53 ± .029	.231	6.54
M_4	L	38	2.8–3.6	3.17 ± .032	.200	6.31
	AW	35	2.6–3.7	2.98 ± .040	.238	7.99
	PW	29	2.0–2.8	2.34 ± .043	.229	9.79
M_{1-3}	L	59	11.2–13.2	12.50 ± .064	.493	3.94

TABLE 18. Statistical data on upper dentitions of *Bettongia lesueur* from Nannup Cave.

		N	OR	Mean ± SE	SD	CV (%)
P^3	L	2	4.86–5.14	5.00	...	...
	W	2	2.74–2.81	2.78	...	...
dP^4	L	2	...	3.72	...	...
	AW	2	2.66–3.12	2.89	...	...
	PW	2	2.96–3.19	3.08	...	...
P^4	L	6	7.75–8.66	8.31	...	...
	AW	6	2.58–2.96	2.76	...	...
	PW	7	2.74–3.19	2.91	...	...
M^1	L	13	3.95–4.71	4.23 ± .050	.18	4.26
	AW	13	3.80–4.26	4.02 ± .039	.14	3.48
	PW	13	4.03–4.60	4.35 ± .053	.19	4.37
M^2	L	12	4.10–4.82	4.47 ± .055	.19	4.25
	AW	12	4.10–4.56	4.38 ± .038	.13	2.97
	PW	12	3.80–4.41	4.18 ± .046	.16	3.83
M^3	L	10	3.42–4.18	3.38 ± .076	.24	6.27
	AW	10	3.27–4.03	3.64 ± .070	.22	6.04
	PW	10	2.81–3.34	3.05 ± .057	.18	5.90
M^4	L	3	2.51–3.12	2.85	...	...
	AW	3	2.36–2.81	2.51	...	...
	PW	3	1.14–2.13	1.50	...	...
M^{1-3}		10	11.85–13.52	12.48 ± .175	.53	4.25
M^{1-4}		3	14.71–15.38	14.96	...	...

TABLE 19. Statistical data on lower dentitions of *Bettongia lesueur* from Nannup Cave.

		N	OR	Mean ± SE	SD	CV (%)
P_3	L	8	4.41–4.94	4.78	...	...
	W	8	2.58–2.89	2.77	...	...
dP_4	L	8	3.24–3.80	3.46	...	...
	AW	7	2.20–2.51	2.32	...	...
	PW	8	2.66–3.04	2.88	...	...
P_4	L	4	6.38–6.84	6.69	...	...
	AW	4	2.51–2.66	2.59	...	...
	PW	4	2.28–2.54	2.39	...	...
M_1	L	13	3.72–4.26	3.96 ± .053	.19	4.80
	AW	13	3.27–3.57	3.42 ± .025	.09	2.63
	PW	13	3.57–4.03	3.82 ± .031	.11	2.88
M_2	L	13	4.03–4.86	4.39 ± .067	.24	5.47
	AW	13	3.95–4.33	4.14 ± .039	.14	3.38
	PW	13	3.88–4.26	4.02 ± .036	.13	3.23
M_3	L	9	3.80–4.33	3.95	...	...
	AW	9	3.80–4.18	4.01	...	...
	PW	9	3.27–3.50	3.39	...	...
M_4	L	1	...	3.04	...	...
	AW	1	...	2.89	...	...
	PW	1	...	1.98	...	...
M_{1-3}	L	9	11.32–12.62	12.10	...	...
M_{1-4}	L	1	...	15.26	...	...

Upper Dentition.—The P^3 is a serrate, bladelike tooth which is aligned with the molar row (fig. 8A–D). It has six grooves on the labial side (table 12). This agrees with the number of five to six reported by Marshall (1973, p. 106) for the P^3s of a Pleistocene sample from Lake Victoria and by Finlayson (1958, p. 256) for the P^3s of a modern population from central Australia. The anterior and posterior crown heights are approximately the same. In crown view the tooth has an even oval shape with prominent cingula.

The dP^4 is roughly square and molariform in structure, with four approximately equal-sized principal cusps (fig. 8A–D). The parastyle is large and laterally compressed and joins with the paracone to form an anterior blade that is aligned with the main ridge of the P^3. The dP^4 usually lacks the mesostyle which is frequently present on the dP^4 of *B. penicillata*, but PM 4786 (fig. 8A,D) has a small mesostyle.

The P^4 is elongate, bladelike, and usually straight, and like the P^3, is aligned with the molar row (figs. 7, 8). It has nine to ten grooves on the labial side (table 12). This agrees with the number of eight to ten reported by Marshall (1973, p. 103) and by Finlayson (1958, p. 266). Tate (1948, p. 266) reported nine grooves for *B. lesueur*. *Bettongia penicillata* is reported by Finlayson (1958) to have seven grooves.

The upper molars are square with four principal cusps. Their size decreases markedly from M^2 to M^4; the relative sizes are $M^2 > M^1 > M^3 > M^4$. This is said by Wakefield (1967) and Tate (1948) to be characteristic of this species.

The protoloph and metaloph are straight, with bulbous expansions on the labial segments. The posterior crest of the protocone and the anterior crest of

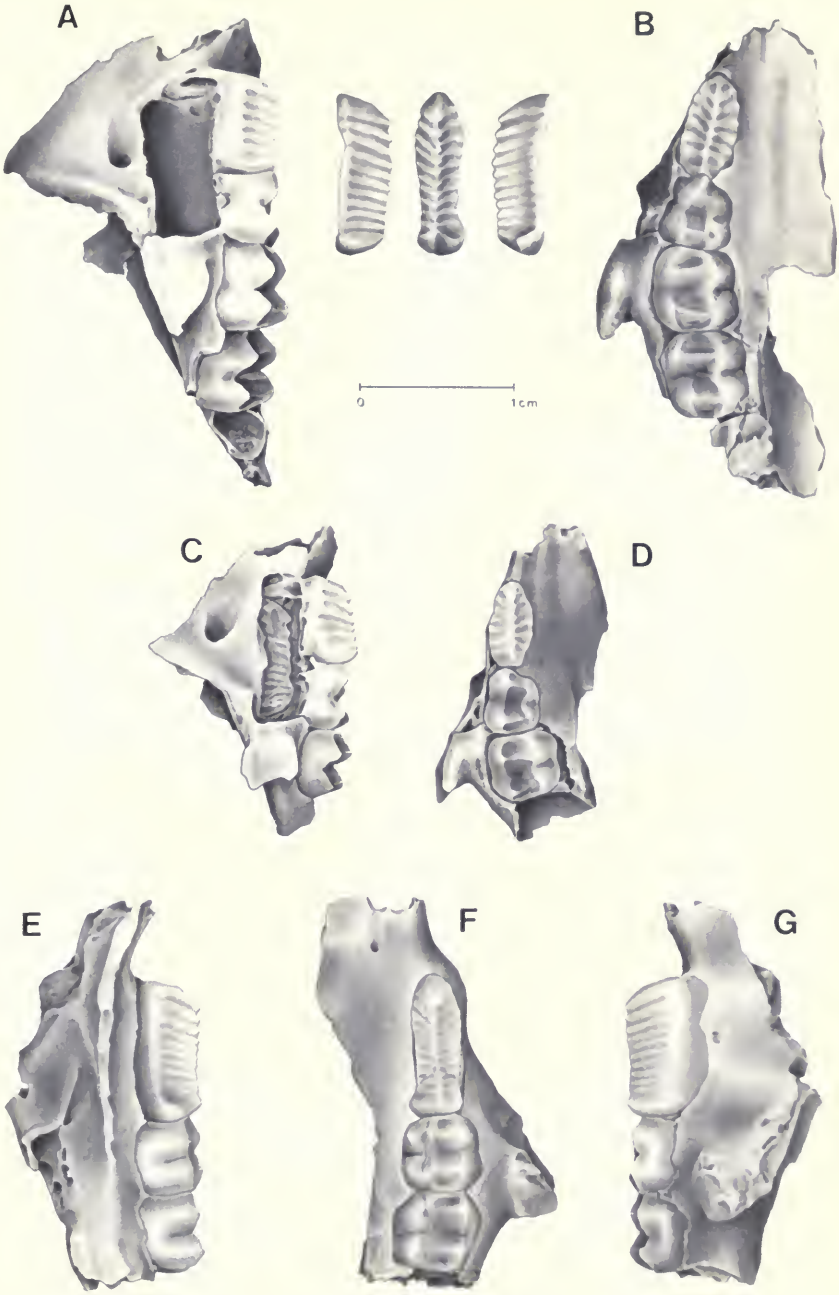

FIG. 8. *Bettongia lesueur* from Madura Cave, Units 1 (post-Pleistocene) and 2 (late Pleistocene). **A,B,** PM 4786, right maxillary with P^3, dP^4, M^{1-2} in place, removed P^4, and crypt for M^3, shown in labial and ventral views. The P^4 is also shown in lingual view. **C,D,** PM 4787, right maxillary fragment with P^3, dP^4, exposed P^4, M^1, and crypt for M^2, shown in labial and ventral views. **E-G,** TMM 41106-117, left maxillary fragment with P^4-M^2, shown in lingual, ventral, and labial views.

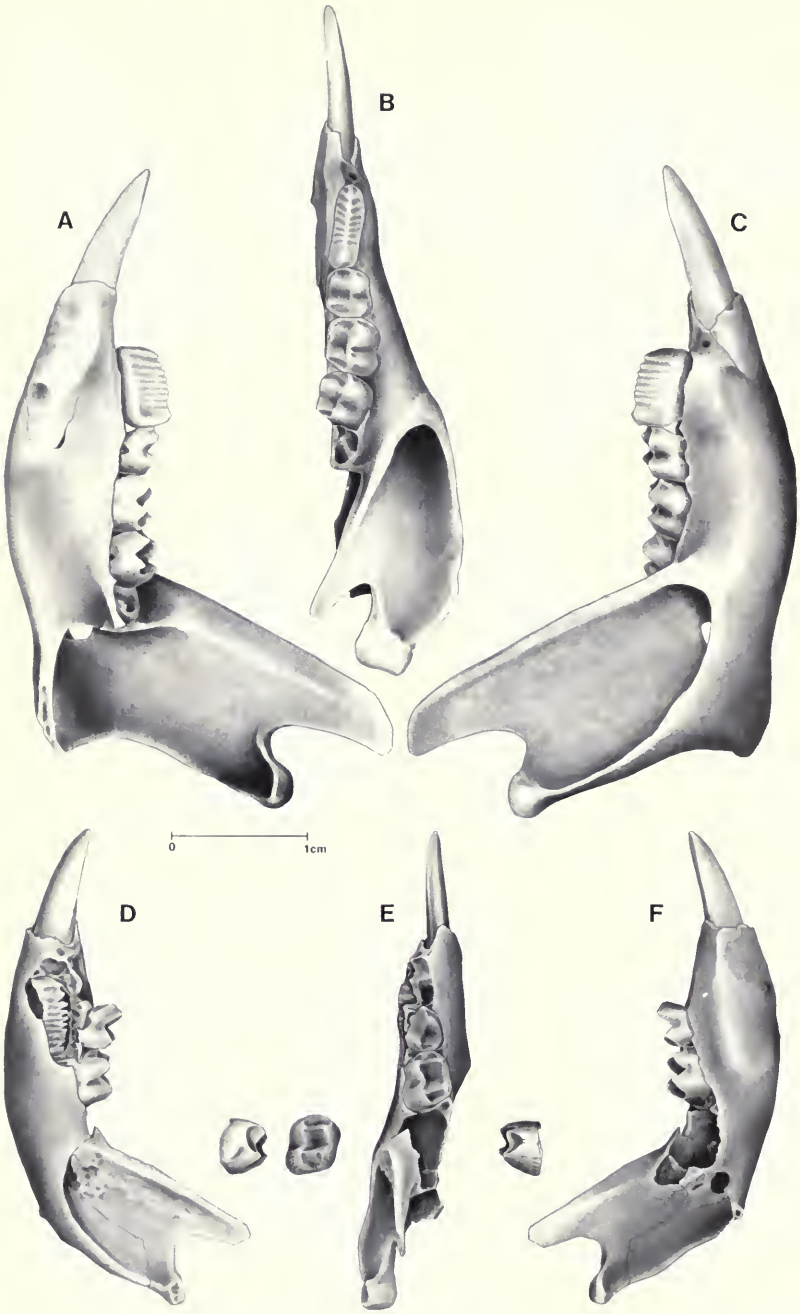

FIG. 9. *Bettongia lesueur* from Madura Cave, surface (Recent) and Unit 1 (post-Pleistocene). **A-C,** TMM 41106-20. Right ramus with I, P_4-M_3, and alveoli for M_4, shown in lingual **(A),** dorsal, and labial views. **D-F,** PM 4795. Left ramus of a juvenile with I, dP_4, P_4 in crypt, M_1, and M_2 removed from crypts, shown in labial **(D),** dorsal, and lingual views. The M_2 is shown in anterior (left), crown, and posterior views.

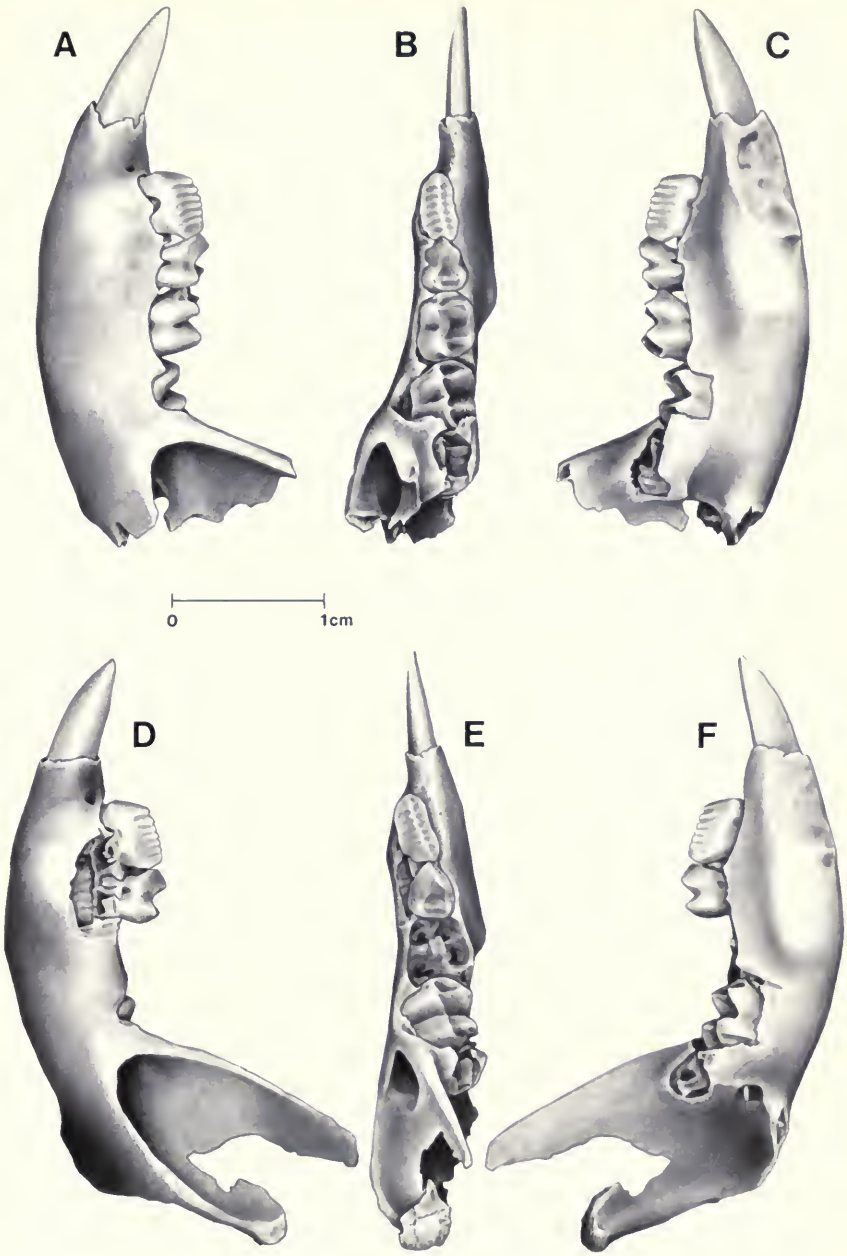

FIG. 10. *Bettongia lesueur* from Madura Cave, surface (Recent) and Unit 1 (post-Pleistocene). **A-C**, TMM 41106-26. Left ramus with I, P_3, P_4 unexposed in crypt, M_1, M_2 erupting, M_3 in crypt, shown in labial **(A)**, dorsal, and lingual views. **D-F**, PM 4796. Left ramus with I, P_3, dP_4, P_4 in crypt, M_1 missing, M_2 erupting, M_3 in crypt, shown in labial **(D)**, dorsal, and lingual views.

the hypocone are thick. They turn into the central basin, where they may or may not join. The inturned crest from the hypocone usually is larger than the one from the protocone. The crests of the paracone and metacone are sharp. They also turn into the central basin, but they do not join. There usually is no mesostyle (Tedford, 1967; Marshall, 1973), but PM 4786 (fig. 8A,B) has a small mesostyle on dP^4 and a trace of one on M^1.

Lower Dentition.—The P_3 is a straight, serrate, bladelike tooth which is aligned with the molar row (fig. 10). In crown view it is somewhat oval, with cingular shelves. One-fourth of our sample has five grooves on P_3; the rest of the specimens have six grooves. This agrees with the five to six grooves reported by Marshall (1973, p. 105) and by Finlayson (1958, p. 256). *Bettongia penicillata* has five grooves on P_3 (Finlayson, 1958). The anterior and posterior crown heights are the same.

The dP_4 (figs. 9D–F, 10) is triangular in crown view because it lacks a protoconid. The metaconid, which is the highest cusp, is laterally compressed and has an anterior bladelike process which is a functional continuation of the P_3. The entoconid is higher than the hypoconid and is joined to it by a hypolophid. The hypoconid is joined to the metaconid by a ridge. A postcingulum borders a small cingular basin.

The P_4 is straight, serrate, and bladelike and is aligned with the molar row (figs. 9, 10). The posterior cusp is laterally compressed and about three times as large as the other cusps on the blade. Crown height is uniform along the entire length of the tooth. The blade has seven to nine grooves, with nine most common. This is slightly less than the eight to ten grooves reported by Marshall (1973, p. 106) and the nine reported by Finlayson (1958, p. 256). *Bettongia penicillata* has seven grooves (Finlayson, 1958).

The lower molars (figs. 9, 10) are rectangular and slightly longer than wide. The M_4 may be triangular because of reduction of the hypolophid. The protolophid is shorter than the hypolophid in M_1, equal in size in M_2, and longer in M_3. The lingual segments of both lophids are swollen. Crests run from the protoconid and hypoconid into the central basin. The metaconid and entoconid are joined by sharp crests at the labial edges of the teeth. The pro- and postcingula are large and outline oval cingular basins.

Discussion

A comparison of dental dimensions of the Madura Cave sample (tables 13–15) with the dental dimensions of fossil samples from Lake Menindee, New South Wales (Tedford, 1967, p. 35), Lake Victoria (Marshall, 1973; tables 16, 17), and Nannup Cave, southwestern Australia (tables 18, 19) and of Recent samples from central Australia and South Australia (Finlayson, 1958, pp. 255, 256, 258, 264; summarized by Tedford, 1967) shows only minor differences. The Madura Cave sample has slightly lower mean values for most measurements than those of the other samples, although the ranges overlap considerably. The exceptions to this rule are the widths of dP^4 and M^2 and the length of dP^4, which have larger mean values than do those of any of the other samples. The Madura Cave sample is closest in size to the samples from Lake Menindee and Lake Victoria.

Only M^1 and M_2 have large enough sample sizes to make calculation of coefficients of variation worthwhile. The coefficients are slightly higher than the

corresponding values for the other samples (tables 13–19), probably because of the small size of the Madura Cave sample.

Size comparisons of the Madura Cave sample with other samples of fossil and recent *B. lesueur* are somewhat uncertain because of the small sample size and wide age range of the Madura Cave material. The Madura Cave sample has smaller average values for most measurements of the upper dentition than do samples from Lake Menindee, Lake Victoria, and Nannup Cave (tables 14, 16, 18; Tedford, 1967, table 7). The samples from Lake Menindee, Lake Victoria, and Nannup Cave are similar in size, but for a number of measurements, the Lake Menindee sample has the highest mean values. The Madura Cave sample also shows smaller mean values than the modern sample from central Australia in the six measures available for comparison (tables 13, 14; Tedford, 1967, table 5).

A decrease in size of modern examples of *B. lesueur* from the humid area of southwestern Australia through southern South Australia to arid central Australia has been reported by Finlayson (1958) and Tedford (1967). This size cline does not seem to exist in the fossil samples. Pleistocene specimens from Lake Victoria and Lake Menindee, both now in the arid zone, are as large as or larger than Pleistocene specimens from Nannup Cave in the humid area of southwestern Western Australia. The Pleistocene specimens from Madura Cave, also now in the arid zone, are as small as or smaller than modern specimens from arid South Australia in spite of other indications that, at that time, the climate in the vicinity of Madura Cave was more humid than it is today.

Bettongia lesueur was distributed through a wide range of environments at the time of European settlement (Finlayson, 1958, p. 240). In the more humid parts of its range, it was sympatric with *B. penicillata*. *Bettongia lesueur* is regarded by Finlayson (1958, pp. 297, 298) as being competitively superior to both *B. penicillata* and *Caloprymnus campestris* in arid areas. This advantage probably is due in part to its burrowing habit, which the other two species lack (Marshall, 1973). The much greater abundance of *B. lesueur* than of *B. penicillata* in the deposits at Lake Menindee (101 *B. penicillata* to five *B. lesueur*; Tedford, 1967) and Lake Victoria (119 *B. penicillata* to two *B. lesueur*; Marshall, 1973) has been attributed by Marshall (1973) to this difference in adaptation to arid conditions. *Caloprymnus* is rare in the Lake Menindee collections (two specimens) and not recorded from Lake Victoria. In contrast, the number of Madura Cave specimens definitely assignable to *B. lesueur* (20) is smaller than the number assignable to *B. penicillata* (38), and *Caloprymnus campestris* is much more abundant than either species of *Bettongia*.

Any attempt to account for these differences in representation of the two species of *Bettongia* in the various samples must consider the fact that the burrowing habit of *B. lesueur* must greatly increase the probability of remains of this species being preserved in open sites such as Lake Menindee and Lake Victoria. The numerous articulated skeletons of *B. lesueur* found at both of these sites and the clumped distribution of bones of *B. lesueur* and of *Lasiorhinus* sp., another communal burrower, at Lake Menindee suggests that many of these animals died in their burrows (Tedford, 1967, p. 23; Marshall, 1973). In contrast, the principal agents for introduction of bones into the Madura Cave deposits were avian and mammalian predators, which would bias the sample differently, but which might more accurately reflect the relative abundance of the living populations in the area.

Bettongia penicillata

Bettongia penicillata Gray, 1837
Hypsiprimnus ogilbyi Waterhouse, 1841
Bettongia gouldi Waterhouse, 1846

Material

Surface pickup
TMM 41106-27, left maxillary with P^3, dP^4, P^4 removed from crypt, M^1, M^{2-3} in crypt, edentulous premaxillary (fig. 13A–C)
Trench 1, Unit 1, top 1 foot
PM 4789, left maxillary with P^3 in crypt, dP^4, P^4 removed from its crypt, M^1, crypt for M^2 (fig. 13G–I)
PM 4792, right ramus with I, P_3, dP_4, P_4 in crypt, M_1 (fig. 14D–F)
PM 4794, left ramus with I, P_3, dP_4, P_4 in crypt, M_1, alveolus for M_2 (fig. 14A–C)
Trench 3, Unit 2, Level ?
TMM 41106-6, left maxillary fragment with worn M^{1-2} (fig. 13D–F)
TMM 41106-62, left P^4
TMM 41106-603, left M^2
TMM 41106-5142, right P^4 fragment
Trench 3, Unit 2, Level 4
PM 38688, left P_4
Trench 3, Unit 2, Level ? or Trench 4, Unit 1
PM 38690, right M^1 or M^2
Trench 4, Unit 1
TMM 41106-533, right P_3
TMM 41106-586, -605, two left M^1s or M^2s
TMM 41106-614, right P^3
TMM 41106-622, right P_3
TMM 41106-623, right P^3
TMM 41106-685, left P^3
TMM 41106-686, right P^3
TMM 41106-5144, broken upper molar
Trench 4, Unit 2, Level 1
WAM 78.3.10, left M^1 or M^2
Trench 4, Unit 2, Level 2
PM 38691, 38692, two left P^3s
Trench 4, Units 4–5
TMM 41106-18, left dP^4
TMM 41106-648, left ramus fragment with P_4–M_1 (fig. 14G–I)
WAM 78.3.12, left P_3
PM 38694, left P_4
PM 38695, right P^3
PM 38696, right P^4
PM 38697, left M^1
PM 38698, right M^2
PM 38701, left dP^4
PM 38703, right M^2 or M^3
PM 38705, left M^1 or M^2
PM 38736, right P^3 or left P_3
PM 38737, right P^3
Trench ?, Unit ?, Level ?
PM 38715, right dP^4

Comparative Material

Recent, southwestern Western Australia
FMNH 35325, 35330

Nannup Cave, southwestern Western Australia
PM 5142, 5143, 5149, 5156, 5159, 5167, 5169, 5172, 5173, 5175–5177, 5222, 5232, 5973, 5974, 5975–5977, 5979, 5981, 5982
Weebubbie Cave, southeastern Western Australia (north of Eucla)
TMM 41107-67
Cave N-31, southwestern South Australia
TMM 41235-97

Description

Skull.—Other than maxillary fragments with teeth, the only skull material is the left side of the facial region of a juvenile skull (TMM 41106-27; fig. 13A–C). Because it is a juvenile, comparisons of cranial characters must be made with caution. The tooth row turns sharply linguad at the level of M^2, suggesting that the tooth rows converged strongly posteriorly. This is a diagnostic character of *B. penicillata* (Finlayson, 1958, p. 284).

Upper Dentition.—The P^3 is a broadly oval tooth with a laterally compressed serrate ridge (fig. 13A–C). The base is bulbous and is widest about at the midpoint. Cingula are absent or weak. The anterior end of the tooth usually is turned outward with respect to the molar row. There are five grooves on the labial surface. The crown is highest at the anterior end. PM 4789 does not fit the foregoing description. It has a more elongate P^3 with a crest which is slightly curved labially at its anterior end. There is a prominent notch in the labial cingulum and the lingual cingulum is prominent, with three cuspules which are placed opposite the three posterior lingual ridges. Although these characters are reminiscent of *B. lesueur*, PM 4789 has been referred to *B. penicillata* because it has seven grooves on the P^4 and mesostyles on dP^4 and M^1.

The dP^4 is molariform. The paracone and parastyle are joined to form a laterally compressed, anteriorly projecting blade which is a functional continuation of the P^3 (fig. 13A–F). Crests from the paracone and metacone and from the protocone and hypocone close the central basin on the labial and lingual sides. Unlike M^{1-3}, dP^4 does not have a spur from the hypocone extending into the central basin. A mesostyle is present in PM 4789 but not in TMM 41106-27 (although this specimen has a mesostyle on M^1). Finlayson (1958) found the mesostyle to be present only rarely on the dP^4s of a sample from central Australia.

The P^4 is elongate, laterally compressed, and serrate (fig. 13A–F). The long axis of the tooth is turned outward anteriorly with respect to the molar row. The crest may be straight or curved labially at the anterior end. Seven grooves are present on the labial side of the blade. The posterointernal cusp is compressed anteroposteriorly, and is two to three times wider than, but lower than, the posterior cusp of the blade. The posterior cusp of the blade usually is turned outward. The tooth is constricted at the middle. The crown is highest at the anterior end.

Of the upper molars (fig. 13), only M^1s and M^2s can be positively assigned to *B. penicillata*. The width of M^1 and M^2 is equal to or slightly greater than the length. The protoloph and metaloph are nearly straight and have less prominent bulges on their labial segments than do the lophs of *B. lesueur*. The lophs and ridges are lower and the central basin is more open than in *B. lesueur*. A mesostyle is present on M^1. It varies from single and minute in TMM 41106-27 to complex and prominent in PM 4789.

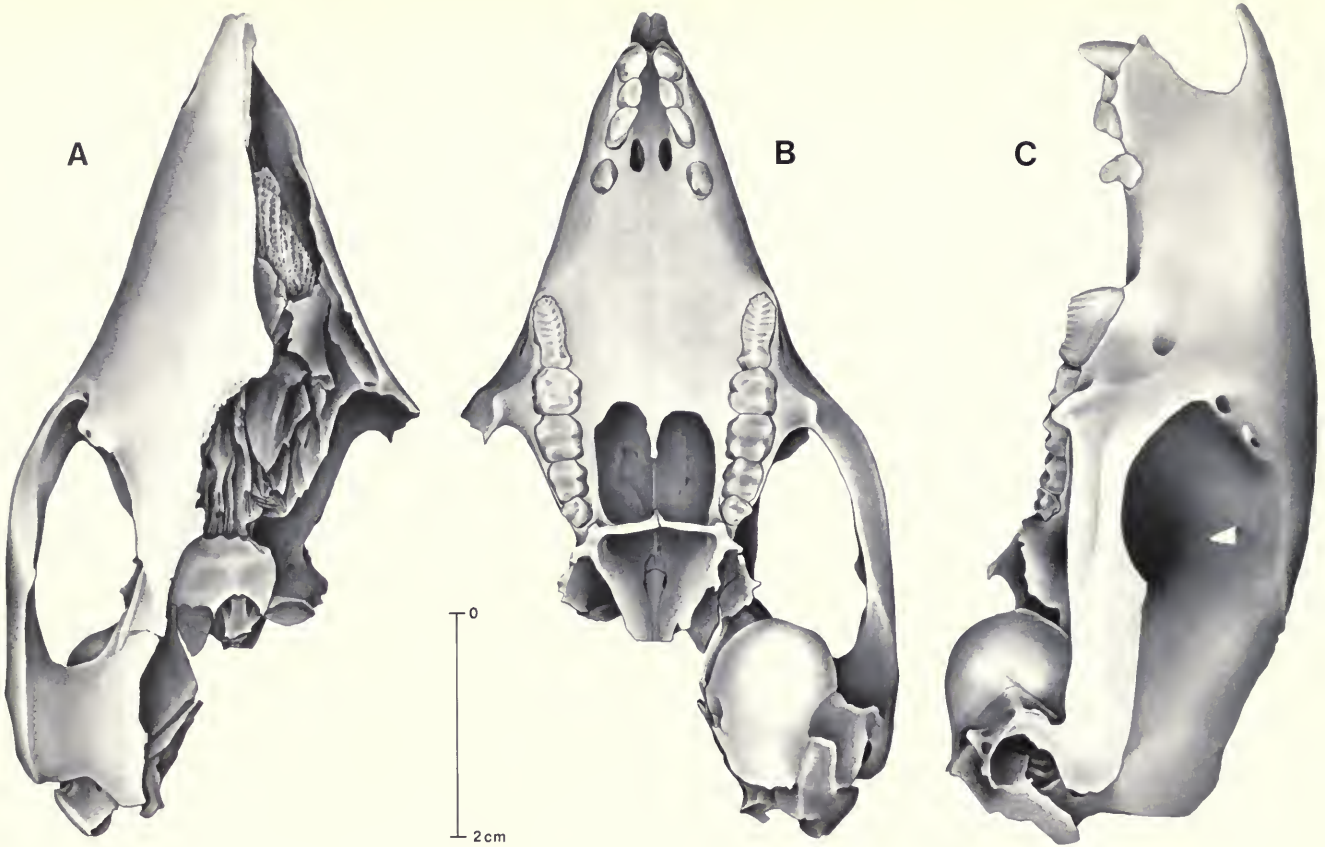
A
B
C
0
2cm

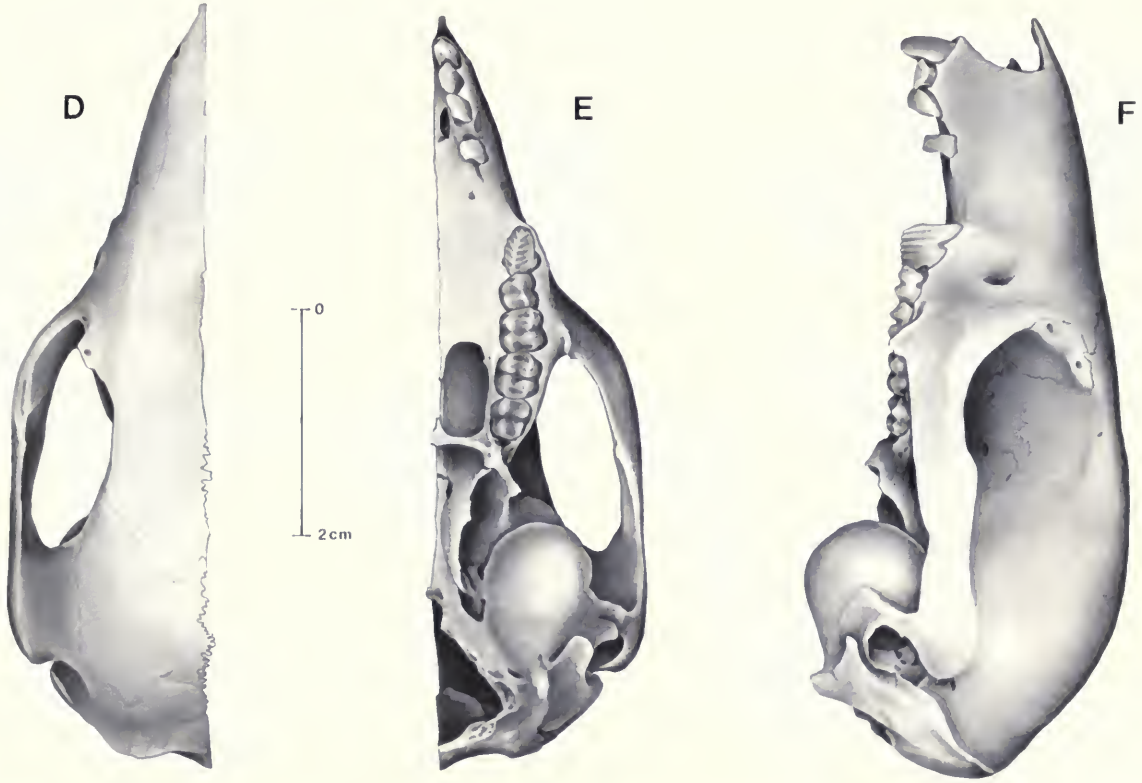

FIG. 11. *Bettongia penicillata*, Recent. **A-C**, FMNH 35325. Skull in dorsal, ventral, and lateral views. **D-F**, FMNH 35330. Skull in dorsal, ventral, and lateral views.

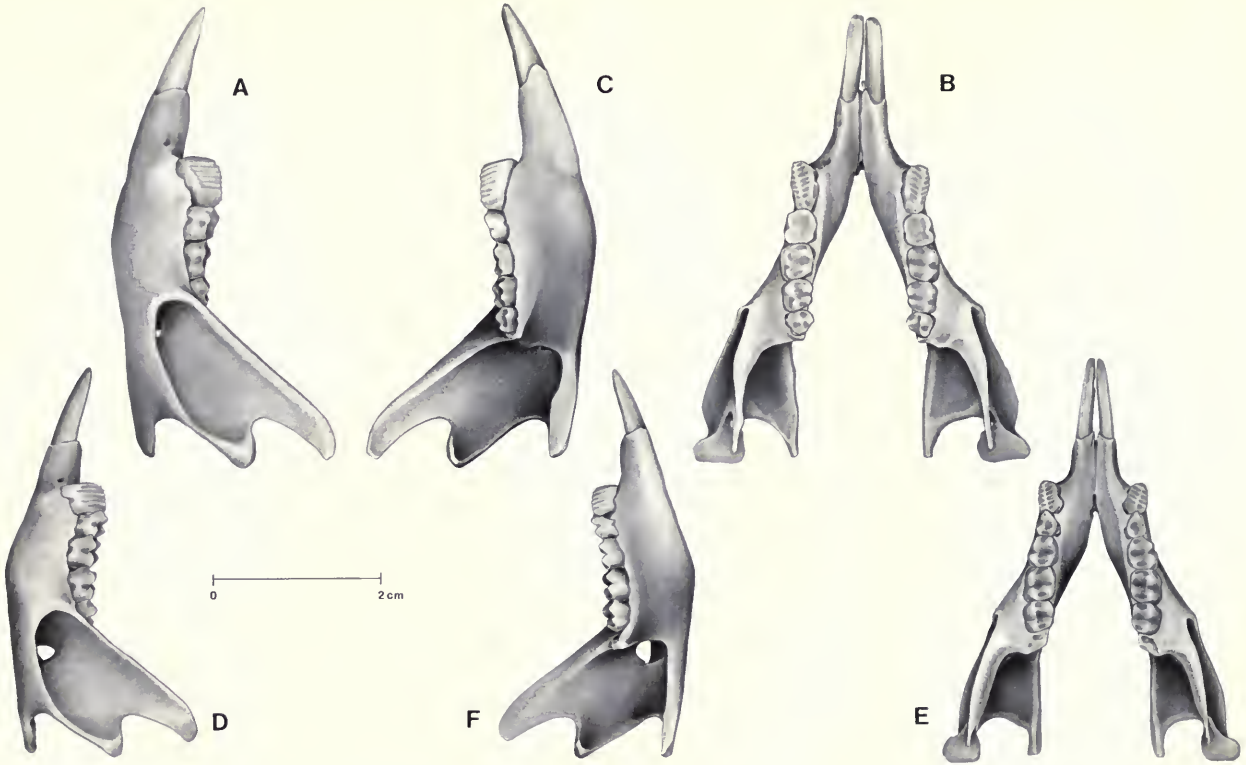

FIG. 12. *Bettongia penicillata*, Recent. **A-C**, FMNH 35325. Left ramus in labial **(A)** and lingual **(C)** views; both rami in dorsal **(B)** view. **D-F**, FMNH 35330. Left ramus in labial **(D)** and lingual **(F)** views; both rami in dorsal **(E)** view.

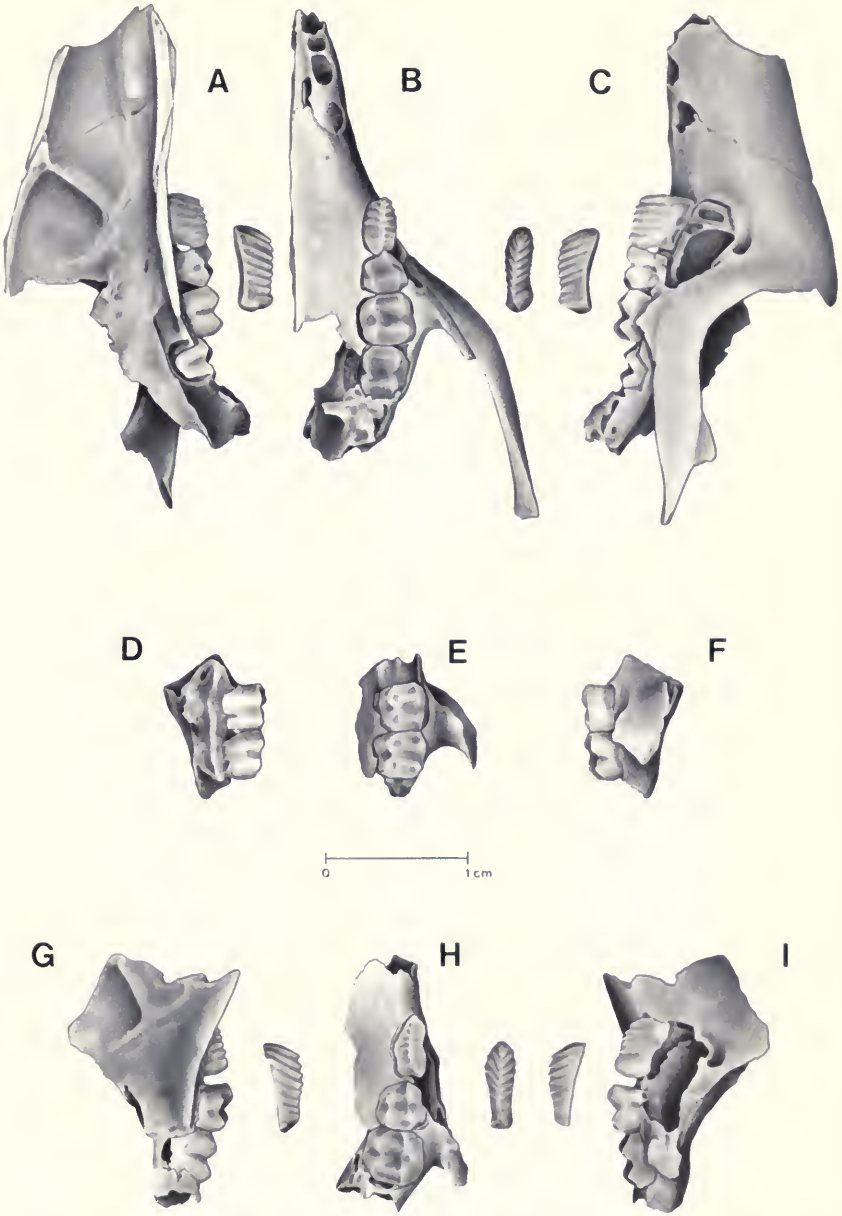

FIG. 13. *Bettongia penicillata* from Madura Cave, surface (Recent) and Unit 1 (post-Pleistocene). **A–C,** TMM 41106-27. Edentulous premaxillary and left maxillary with P^3, dP^4, P^4 removed from crypt, M^1, M^2, M^3 in crypt, shown in lingual **(A),** ventral, and labial views (each with inset of P^4). **D–F,** TMM 41106-6. Left maxillary fragment with M^1, M^2, shown in lingual **(D),** ventral, and labial views. **G–I,** PM 4789. Left maxillary fragment with partly erupted P^3, dP^4, P^4 removed from crypt, M^1, crypt for M^2, shown in lingual **(G),** ventral, and labial views (each with inset of P^4).

TABLE 20. Statistical data on upper dentitions of *Bettongia penicillata* from Madura Cave compared with other fossil and modern samples.

		Madura Cave					Nannup Cave					Lake Victoria*		Recent Victoria*			Recent Western Australia	
		N	OR	Mean ± SE	SD	CV (%)	N	OR	Mean ± SE	SD	CV (%)	P 29425	P 29426	C 6899	C 6900	C 6901	FMNH 35325	FMNH 35330
P^3	L	11	3.95–4.64	4.33 ± .072	.24	5.54	1	...	4.71	...	...	...	...	...	...	...	...	4.33
	W	11	2.20–2.58	2.43 ± .033	.11	4.53	1	...	2.74	...	...	...	...	...	...	...	...	2.78
dP^4	L	2	2.89–3.34	3.12	...	...	1	...	3.19	...	...	...	3.5	...	3.0	3.6	...	3.27
	AW	2	2.28–2.89	2.59	...	...	1	...	2.62	...	...	...	2.9	...	2.6	2.8	...	2.81
	PW	2	2.66–3.34	3.00	...	...	1	...	3.04	...	...	...	3.3	...	3.0	3.4	...	3.27
P^4	L	2	5.78–6.00	5.89	...	...	9	6.54–7.52	7.00 ± .097	.29	4.14	...	...	...	...	...	6.96	...
	AW	2	1.98–2.20	2.09	...	...	10	2.74–3.19	2.89 ± .054	.17	5.88	...	...	...	...	...	2.96	...
	PW	2	1.67–1.90	1.79	...	...	11	2.51–3.04	2.73 ± .063	.21	7.69	...	...	...	...	...	2.92	...
M^1	L	3	3.19–3.88	3.50	...	...	13	3.88–4.18	3.98 ± .028	.10	2.51	3.9	4.1	4.2	3.7	4.1	4.26	3.99
	AW	3	3.34–4.07	3.64	...	...	13	3.80–4.26	4.09 ± .039	.14	3.42	4.0	4.2	4.2	3.7	4.0	4.22	4.10
	PW	3	3.34–4.07	3.66	...	...	13	3.95–4.33	4.20 ± .033	.12	2.86	4.1	4.3	4.0	3.7	4.0	4.22	4.18
M^2	L	2	3.34–3.57	3.46	...	...	13	3.95–4.48	4.16 ± .044	.16	3.85	4.2	4.5	4.1	3.9	...	4.28	4.18
	AW	2	3.46–3.57	3.52	...	...	13	3.95–4.48	4.25 ± .047	.17	4.00	4.5	4.5	4.0	3.9	...	4.37	4.26
	PW	2	3.23–3.27	3.25	...	...	13	3.80–4.26	4.07 ± .039	.14	3.44	4.3	4.2	3.7	3.6	...	4.03	4.14
M^3	L	...	...	...	...	...	8	3.34–3.88	3.63	...	...	4.0	...	3.7	3.6	...	3.65	3.80
	AW	...	...	...	...	...	8	3.50–3.92	3.62	...	...	4.1	...	3.5	3.2	...	3.57	3.76
	PW	...	...	...	...	...	8	2.81–3.42	3.14	...	...	3.5	...	2.9	3.7	...	3.04	3.19
M^4	L	...	...	...	...	...	2	2.20–2.51	2.36	...	...	2.5	...	2.7	...	...	2.43	...
	AW	...	...	...	...	...	2	...	2.28	...	...	2.7	...	2.5	...	...	2.58	...
	PW	...	...	...	...	...	2	1.67–1.82	1.75	...	...	2.3	...	2.0	...	...	1.90	...
M^{1-3}	L	...	...	...	...	...	8	11.35–12.31	11.74	...	...	...	...	...	...	...	12.11	11.63
M^{1-4}	L	...	...	...	...	...	2	13.65–14.19	13.92	...	...	...	...	...	...	...	14.36	...

* Data from Marshall, 1973.

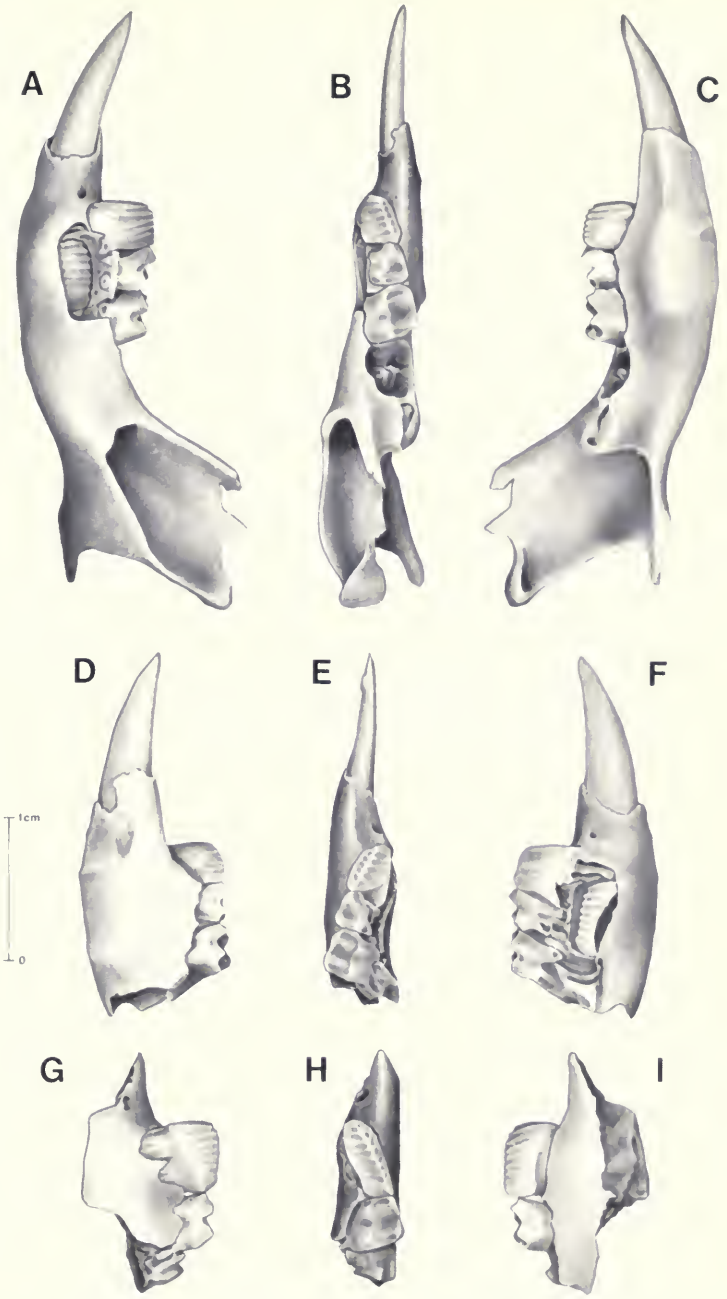

FIG. 14. *Bettongia penicillata* from Madura Cave, Unit 1 (post-Pleistocene). **A-C**, PM 4794. Left ramus with I, P_3, dP_4, P_4 in crypt, M_1, alveoli for M_2, M_3 in crypt, shown in labial **(A)**, dorsal, and lingual views. **D-F**, PM 4792. Right ramus with I, P_3, dP_4, P_4 in crypt, M_1, shown in lingual **(D)**, dorsal, and labial views. **G-I**, TMM 41106-648. Left ramus fragment with P_4, M_1, shown in labial **(G)**, dorsal, and lingual views.

TABLE 21. Statistical data on lower dentitions of fossil and living samples of *Bettongia penicillata*.

		Madura Cave			Nannup Cave					Recent Western Australia	
		N	OR	Mean	N	OR	Mean ± SE	SD	CV (%)	FMNH 35325	FMNH 35330
P_3	L	5	3.57–4.18	3.91	5	3.57–4.64	4.07	...	...	...	4.18
	W	5	2.13–2.89	2.49	5	2.36–2.58	2.48	...	...	...	2.58
dP_4	L	2	2.66–2.89	2.78	3	2.89–3.08	3.00	...	...	...	3.34
	AW	2	1.71–2.24	1.98	3	2.32–2.43	2.37	...	...	...	2.13
	PW	2	2.13–2.58	2.36	3	1.82–1.90	1.85	...	...	...	3.74
P_4	L	...	...	...	3	6.00–6.61	6.36	...	...	6.69	...
	AW	...	...	...	3	2.74–2.89	2.84	...	...	2.96	...
	PW	...	...	...	2	2.28–2.74	2.51	...	...	2.43	...
M_1	L	2	3.19–3.46	3.33	9	3.57–4.10	3.77 ± .057	.17	4.51	4.18	4.03
	AW	2	2.81–3.12	2.97	9	3.19–3.57	3.33 ± .047	.14	4.20	3.80	3.34
	PW	2	3.04–3.34	3.19	9	3.34–3.95	3.66 ± .060	.18	4.92	3.88	3.72
M_2	L	...	...	...	9	3.88–4.41	4.08 ± .053	.16	3.92	4.48	4.18
	AW	...	...	...	9	3.57–4.10	3.88 ± .053	.16	4.12	4.18	3.80
	PW	...	...	...	9	3.42–4.03	3.79 ± .080	.24	6.33	3.88	3.57
M_3	L	...	...	...	6	3.57–4.03	3.76	...	...	3.84	3.34
	AW	...	...	...	6	3.27–4.03	3.69	...	...	3.76	3.80
	PW	...	...	...	6	3.00–3.80	3.36	...	...	3.23	3.38
M_4	L	...	...	...	1	...	2.74	...	...	2.96	...
	AW	...	...	...	1	...	2.74	...	...	3.04	...
	PW	...	...	...	1	...	1.67	...	...	1.90	...
M_{1-3}	L	...	...	...	6	11.02–12.00	11.48	...	...	12.39	11.55
M_{1-4}	L	...	...	...	1	...	14.75	...	...	15.21	...

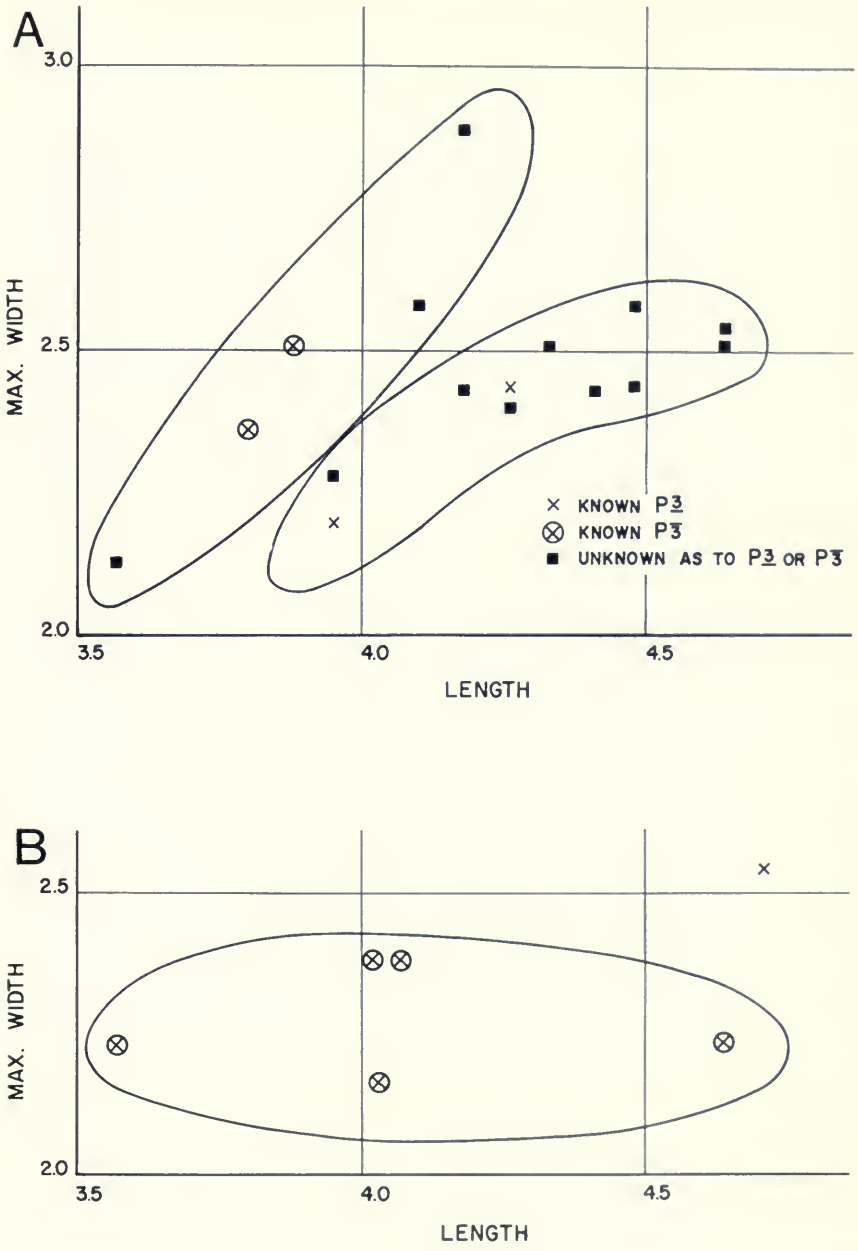

FIG. 15. Bivariate graphs of P^3s and P_3s of *Bettongia penicillata* from Madura Cave and Nannup Cave. **A**, Plot of P^3s and P_3s from Madura Cave, showing probable assignment. **B**, Plot of length vs. maximum width of P_3s and one P^3 of *Bettongia penicillata* from Nannup Cave. Note the apparent reversal of position of the scatters of the two teeth. Symbols as in **A**.

Lower Dentition.—The dP_4 is triangular and lacks a protoconid (fig. 14A–F). The metaconid is the highest cusp; it is laterally compressed and projects forward to the posterior end of the P_3. The entoconid is higher than the hypoconid and is joined to it by a hypolophid. The metaconid and entoconid are connected by a ridge. The posterior cingulum is small.

The P_4 is a simple, laterally compressed blade with a straight crest (fig. 14). The posterointernal cusp is either absent or reduced to a bulge on the lingual side of the posterior ridge. The long axis of the tooth is turned outward anteriorly with respect to the molar row. There are seven grooves on the labial side of the blade. The anterior part of the tooth is widest. As with P^4, crown height is greatest at the anterior end of the tooth.

Lower molars which are associated with sectorial premolars and which thus can be positively identified as *B. penicillata* are rare in the Madura Cave materials. Only TMM 41106-648, PM 4792, and PM 4794 have M_1 in place (fig. 14). The protolophid of the M_1 is shorter than the hypolophid. The ridge which joins the protoconid and hypoconid is less prominent than it is in *B. lesueur*. The lophids of M_1 are less bulbous than those of *B. lesueur*, and thus the central basin is more open.

Discussion

The P^3 and P_3 of *B. penicillata* are so similar that differentiation of isolated teeth is difficult. The length/width ratios of the four specimens which are still in a maxillary or ramus differ between P^3 (.56, .57) and P_3 (.65, .69). The length/width ratios of the isolated teeth tend to cluster around those of known position, but there is no clear separation between the two groups. A bivariate scatter diagram of length versus width does suggest a separation into two groups which correspond to the groups formed on the basis of length/width ratios (fig. 7A). This is the tenuous basis for the identifications of isolated P3s in this paper. The plots of points representing each tooth are so close to each other that a larger sample size might produce a wide zone of overlap.

A scatter diagram of length versus width for a sample of P3s of *B. penicillata* from a late Pleistocene fauna from Nannup Cave in southwestern Australia (fig. 7B) yields a very different distribution. Even so, it appears that the Nannup Cave P3s might be separable on this basis. The difference between the two samples indicates that criteria for distinguishing between isolated P^3s and P_3s will have to be developed independently for each sample.

Bettongia Species Indet.

Material

Trench 3, Unit 2, Level ?

TMM 41106-116, right ramus fragment with M_{2-3}, alveoli for P_4, M_1, and M_4

TMM 41106-602, right M_2

TMM 41106-681, right M^3 (possibly *Potorous platyops*)

PM 38687, right dP_4 (probably *B. lesueur*)

PM 38716, right ramus fragment with unerupted M_2 in crypt, proximal tip of alveolus for I, alveoli for posterior roots of dP_4, posterior end of crypt for P_4, alveoli for M_1, small crypt for M_3

PM 38717, left dP^4

Trench 3, Unit 2, Level 2
PM 38774, right M^4
Trench 3, Unit 2, Level 4
PM 38689, left M_1
Trench 4, Unit 1, Level ?
TMM 41106-564, left dP^4
TMM 41106-565, right dP_4
TMM 41106-567, -569, two right M_1s
TMM 41106-571, broken right P^4
TMM 41106-572, broken upper molar
TMM 41106-574, right M_2
TMM 41106-578, left M_2 or M_3
TMM 41106-582, broken right upper molar or dP^4
TMM 41106-591, left lower molar
TMM 41106-592, right M_1
TMM 41106-595, left M^3
TMM 41106-596, left M_2
TMM 41106-597, -599, two right M_2s
TMM 41106-601, right M_1
TMM 41106-604, right I_1 fragment
TMM 41106-606, right dP^4
TMM 41106-607, left M_2 or M_3
TMM 41106-608, left dP^4 (probably *B. penicillata*)
TMM 41106-610, right M_1
TMM 41106-615, posterior half right P^3 (probably *B. penicillata*)
TMM 41106-616, left M_1
TMM 41106-617, left M_2
TMM 41106-618, posterior half left P^3 (probably *B. penicillata*)
TMM 41106-620, right M_1
TMM 41106-621, left M_2 or M_3
TMM 41106-2828, left P_3
TMM 41106-5143, upper molar (probably *B. lesueur*)
TMM 41106-5145, left dP^4 (probably *B. penicillata*)
PM 38719, right M_2 or M_3
PM 38720, left upper molar
PM 38752, anterior half ?upper premolar
PM 38753–38756, four right I^1s
PM 38757–38760, four I^3s
PM 38761–38768, eight I^2s
Trench 4, Unit 2, Level 1
WAM 78.3.9, right M_1
WAM 78.3.11, right dP^4 (probably *B. penicillata*)
WAM 78.3.13, right M^3
WAM 78.3.14, dP^4 (possibly not *Bettongia*)
WAM 78.3.15, M^3 or M^2
WAM 78.3.16, right M^2
PM 38709, broken left dP^4
PM 38724, right M_1 or M_2
PM 38725, right M_1
PM 38726, right M_2
PM 38728, left dP^4 (probably *B. lesueur*)
PM 38729, left dP^4 or M^1
PM 38730, broken right molar
PM 38769, edentulous maxillary fragment
Trench 4, Unit 2, Level 2
PM 38710, 38711, two left dP^4s
PM 38731, right M^2
PM 38732, right M^3 or M^2
PM 38733, left M^2 or M^1
PM 38734, left M_3
PM 38735, left M_1

Trench 4, Unit 2, Level ?
PM 38693, ramus fragment with dP_4–M_1 (probably *B. penicillata*)
PM 38770, right M_1
PM 38771, left maxillary with shattered tooth roots
Trench 4, Units 4 and 5
WAM 78.3.17, right M_1
WAM 78.3.18, left M^1
WAM 78.3.19, right M_3
PM 36983–36985, three left I^1s
PM 36986, ?I^1 (possibly other potoroine or phalangerid)
PM 36987, I^2 (possibly other potoroine or phalangerid)
PM 36988, left I^3 (possibly other potoroine)
PM 38699, left M_2 or M_3
PM 38700, broken right M_2
PM 38702, right M_1 or M_2
PM 38704, right M_2
PM 38706, left M_2
PM 38738, broken molar
PM 38739, right M_2
Trench 4, Unit 7, Level 2
PM 38707, right M^2
PM 38708, right M_2 or M_1
PM 38742, left M^2
PM 38743, right M^3
PM 38773, left upper molar
Trench 5, Unit 6
TMM 41106-629, left M^4
TMM 41106-636, left dP^4
TMM 41106-643, right dP^4
TMM 41106-5146, left dP^4
PM 38744, right I_1
PM 38745, left M_2 or M_3
PM 38746, right M^1 or M^2
PM 38747, left M^2
PM 38748, right M_1
PM 38749, right M^1 or M^2
PM 38750, left M^2
PM 38751, left M^2 or M^3
Trench, Unit, and Level data lost
PM 38713, broken right P^4
PM 38714, left M^2

CONCLUSIONS

The Madura Cave deposits contain four species of Potoroinae, *Potorous platyops, Caloprymnus campestris, Bettongia lesueur,* and *Bettongia penicillata. Potorous platyops* and *Caloprymnus campestris* are not known to have occupied the Nullarbor Plain since the beginning of European settlement, although there is an early report of *Caloprymnus campestris* by Tate (1879) with no supporting evidence. The only part of Australia where four species of potoroines have been reported as living animals is a small area near Albany in southwestern Australia. The species reported there are *Potorous tridactylus, P. platyops, Bettongia lesueur,* and *B. penicillata. Potorous platyops* was known as a living animal from two localities in southwestern Western Australia, one near the town of Goomalling (Calaby, 1954), and the other near the Pallinup River, 110 km northeast of Albany (Ride, 1970). Both localities are in areas of higher average annual rainfall (20 to 30 inches [50 to 75 cm]) than the Madura Cave area, which has an

average annual rainfall of approximately 10 inches (25 cm). *Caloprymnus campestris* has been reported from an extremely arid area in central Australia (Finlayson, 1932). The increased diversity of potoroines and the presence of now allopatric species of that group are similar to the situation seen in the Dasyuridae from this site (Lundelius & Turnbull, 1978). This supports the interpretation, based on the dasyurid assemblage, of a climate with more available moisture and more equability than the present climate in this area. The presence of all four potoroines in Unit 1 (C^{14} date of 7470 ± 120 BP from the top 1 foot) demonstrates that the change that resulted in the loss of *Caloprymnus* and *Potorous* took place some time during the last 7,500 years. This is consistent with the conclusions regarding the changing climatic conditions which were made in the earlier parts of this study based on Dasyuridae, Peramelidae, and Phalangeridae.

ACKNOWLEDGMENTS

In addition to those individuals mentioned in earlier parts of this faunal report, we wish to thank Dr. Larry Marshall of the University of Arizona for allowing us to use his unpublished data on *Bettongia penicillata* and *B. lesueur* from Lake Victoria, Mr. Zbigniew Jastrzebski for illustrations, and Ms. Elizabeth Moore and Ms. Melissa Winans for typing and editing.

Financial support was provided by Field Museum of Natural History, the Geology Foundation of the University of Texas at Austin, and by grants GB 975, GB 3729, and GB 7662 from the National Science Foundation.

LITERATURE CITED

ABBIE, A. A. 1939. Masticatory adaptation peculiar to some diprotodont marsupials. Proc. Zool. Soc. London, **109**: 261–279, 9 figs.

ARCHER, M. 1972. Nullarbor, 1969. The Western Caver, **12**(1): 17–24.

———. 1974. New information about the Quaternary distribution of the thylacines (Marsupialia: Thylacinidae) in Australia. J. Roy. Soc. West. Aust., **57**(2): 43–50.

BUTLER, W. H., AND D. MERRILEES. 1971. Remains of *Potorous platyops* (Marsupialia: Macropodidae) and other mammals from Bremer Bay, Western Australia. J. Roy. Soc. West. Aust., **54**(2): 53–58.

CALABY, J. H. 1954. Comments on Gilbert's notebook on marsupials. West. Aust. Nat., **4**: 147–148.

DESMAREST, A. G. 1804. Nouveau Dictionaire d'Histoire Naturelle, **1**, p. 20.

FINLAYSON, H. H. 1932. *Caloprymnus campestris*. Its recurrence and characters. Trans. Roy. Soc. S. Aust., **56**: 148–167.

———. 1938. On a new species of *Potorous* (Marsupialia) from a cave deposit on Kangaroo Island, South Australia. Trans. Roy. Soc. S. Aust., **62**(1): 132–140, pls. V–VII.

———. 1957. Preliminary description of two forms of *Bettongia* (Marsupialia). Ann. Mag. Nat. Hist., **10**, ser. 12: 552–554.

———. 1958. On central Australian mammals. Part III. The Potoroinae. Rec. S. Aust. Mus. (Adelaide), **13**: 235–302.

GOULD, J. 1840. Description of a new species of *Hypsiprymnus* (*H. graii*). Proc. Zool. Soc. London, **1840**, part VIII, p. 178.

———. 1843. A new species of kangaroo-rat, *Bettongia campestris*. Proc. Zool. Soc. London, **1843**, part XI, p. 81.

———. 1844. Exhibition and character of animals collected by Gilbert, etc. Proc. Zool. Soc. London, **1844**, part XII, p. 103.

GRAY, J. E. 1837. Descriptions of some new or little known Mammalia, in the British Museum. Mag. Nat. Hist. (Charlesworth), **1:** 577–587.

———. 1841. Contributions toward geographical distribution of the Mammalia of Australia, etc., pp. 397–414. *In* Grey, G., Journals of Two Expeditions of Discovery in North-West and Western Australia, Appendix C. T. & W. Boone, London.

LOWRY, J. W. J., AND D. MERRILEES. 1969. Age of the desiccated carcass of a thylacine (Marsupialia, Dasyuroidea) from Thylacine Hole, Nullarbor Region, Western Australia. Helictite, **7**(1): 15–16.

LUNDELIUS, ERNEST L., JR. 1957. Additions to knowledge of the ranges of Western Australian mammals. West. Aust. Nat., **5:** 173–182.

———. 1960. Post-Pleistocene faunal succession in Western Australia and its climatic interpretation. Proc. 21st Int. Geol. Congr., **4:** 142–153.

———. 1963. Vertebrate remains from the Nullarbor Caves. J. Roy. Soc. West. Aust., **46,** pt. 3: 75–80.

LUNDELIUS, ERNEST L., JR., AND WILLIAM D. TURNBULL. 1973. The mammalian fauna of Madura Cave, Western Australia. Part I. Fieldiana: Geol., **31**(1): 1–35.

———. 1975. The mammalian fauna of Madura Cave, Western Australia. Part II. Fieldiana: Geol., **31**(2): 37–117.

———. 1978. The mammalian fauna of Madura Cave, Western Australia. Part III. Fieldiana: Geol., **38:** 1–120.

———. 1981. The mammalian fauna of Madura Cave, Western Australia. Part IV. Fieldiana: Geol., n.s., no. 6: 1–72.

———. 1982. The mammalian fauna of Madura Cave, Western Australia. Part V: Diprotodonta (Part). Fieldiana: Geol., n.s., no. 11: 1–32.

MARSHALL, LARRY G. 1973. The Lake Victoria local fauna: A late Pleistocene-Holocene fauna from Lake Victoria, southwestern New South Wales, Australia. Unpubl. M.A. Thesis, Monash Univ., Clayton, Victoria, Australia.

MATSCHIE, P. 1916. Die Verbreitung der Beutelier auf Neuginea. Mitt. Zool. Mus. Berlin, viii, **2,** p. 257–309.

PARTRIDGE, J. 1967. A 3,300 year old Thylacine (Marsupialia, Thylacinidae), Australia. J. Roy. Soc. West. Aust., **50:** 57–59.

QUOY, J., AND P. GAIMARD. 1824. Voyage de l'Uranie . . . Zoologie, **56.** *In* Freycinet, L. de, Voyage autour du Monde. Chez Pillet Aîné, Paris, 712 pp.

RIDE, W. D. L. 1970. A guide to the native mammals of Australia. Oxford University Press, London, 249 pp.

SMITH, M. 1971. Small fossil vertebrates from Victoria Cave, Naracoorte, South Australia. I. Potoroinae (Macropodidae), Petauridae and Burramyidae (Marsupialia). Trans. Roy. Soc. S. Aust., **95**(4): 185–198.

STIRTON, R. A. 1963. A review of the macropodid genus *Protemnodon.* Univ. Calif. Publ. Geol. Sci., **44**(2): 97–162, 15 figs.

TATE, G. H. H. 1948. Studies on the anatomy and phylogeny of the Macropodidae (Marsupialia). Bull. Am. Mus. Nat. Hist., **91**(2): 235–351.

TATE, RALPH. 1879. The natural history of the country around the head of the Great Australian Bight. Trans Roy. Soc. S. Aust., **2:** 94–128.

TEDFORD, RICHARD H. 1967. The fossil Macropodidae from Lake Menindee, New South Wales. Univ. Calif. Publ. Geol. Sci., **64:** 1–156.

THOMAS, O. 1888. Catalogue of the Marsupialia and Monotremata in the Collection of the British Museum (Natural History), pp. 121–122. London, pp. i–xii + 1–401, pls. I–XXVIII.

WAKEFIELD, N. 1964. Mammal remains, Appendix 1. *In* Mulvaney, D. J., G. H. Lawton, and C. R. Twidale, Archeological excavation of Rock Shelter No. 6, Fromm's Landing, South Australia. Proc. Roy. Soc. Victoria, **77:** 494–498.

———. 1967. Some taxonomic revision in the Australian marsupial genus *Bettongia* (Macropodidae), with a description of a new species. Victorian Nat., **84**(1): 8–22.

WATERHOUSE, G. R. 1841. The natural history of Marsupialia or pouched animals. *In*

Jardine, W., ed., The Naturalist's Library, Marsupials (vol. 30 of the whole series). W. H. Lizars, Edinburgh, 323 pp.

———. 1842. On two new species of the Marsupialia or pouched mammals. Proc. Zool. Soc. London, **1842**, part X, pp. 47–48.

———. 1846. Nat. Hist. Mammals, **1**, 533 pp.

Field Museum of Natural History
Roosevelt Road at Lake Shore Drive
Chicago, Illinois 60605-2496
Telephone: (312) 922-9410